Science Advances

Supplementary Materials for

Rural land abandonment is too ephemeral to provide major benefits for biodiversity and climate

Christopher L. Crawford *et al.*

Corresponding author: Christopher L. Crawford, ccrawford@princeton.edu

This PDF file includes:

Supplementary Text
Figs. S1 to S29
Tables S1 to S6
References

Supplementary Text
Section S1. Extended Results

S1.1 Summary statistics

On average, we found that cropland abandonment lasted for only 14.22 years (SD = 1.44 years) across our time series at our eleven sites (Table S1). Note, however, that these summary statistics are calculated based on the mean abandonment duration at each site, in order to account for different site sizes. The summary statistics reported above and in the main text are therefore the mean of the individual mean abandonment duration values for each of our 11 sites, and the corresponding standard deviation of these individual mean abandonment duration values. This standard deviation represents the variation in mean abandonment duration among sites. For comparison, we also calculated the standard deviation of abandonment duration values at each individual site, which represents the variation among instances of abandonment at that particular site. The mean of these 11 standard deviation values was 7.69 years. These values, along with the mean and standard deviation across the 11 site summary values, are presented in Tables S2-S4.

S1.2 Limited abandonment in Mato Grosso

Mato Grosso, Brazil, was the only site that did not experience substantial amounts of cropland abandonment during our time series (see Table S1). This is unsurprising given the recent history of agriculturally-driven land-use change in Mato Grosso over the last few decades. Moreover, the abandonment that did take place in Mato Grosso was subject to relatively quick recultivation, with half-lives ranging from 11.53 to 18.9 years across our full range of endpoints (Fig. S17). These half-lives were the shortest of any of our sites. However, because Mato Grosso showed large amounts of new cultivation over the course of our time series and relatively little abandonment (11,277 ha, or only 0.59% of the total cropland extent, as of 2017; Table S1), these results should be interpreted with care. In Mato Grosso, agricultural expansion is undoubtedly the dominant force affecting biodiversity and carbon stocks.

S1.3 Biomes

Our sites cover a range of biomes (Fig. S10), as delineated by the Ecoregions2017 map (*79*), including:

- Temperate Broadleaf and Mixed Forests (Vitebsk Belarus/Smolensk, Russia; Bosnia & Herzegovina; Wisconsin, USA),
- Temperate Grasslands, Savannas, and Shrublands (Nebraska/Wyoming, USA; Orenburg, Russia/Uralsk, Kazakhstan; Volgograd, Russia),
- Tropical Grassland (Goiás and Mato Grosso, Brazil),
- Tropical Moist Broadleaf Forests (Chongqing, China; Mato Grosso, Brazil),
- Montane Grassland and Shrublands (Shaanxi/Shanxi, China), and
- Deserts & Xeric Shrublands (Iraq).

Individual ecoregions from the Ecoregions2017 layer are shown in Fig. S12, and the broad categorization of these biomes into forest and non-forest is shown in Fig. S11.

The long-term land-cover outcomes for abandoned croplands (as of 2017) are shown in Fig. S23. Land-cover outcomes for abandoned croplands showed wide variation across sites, with the majority of abandonment in Wisconsin being classified as forest by 2017 (61% forest, 39% grassland), while most abandonment remained in grassland at our other sites (Fig. S23). This limited regrowth of woody vegetation may be a product of the biome (the four sites with the highest proportion of abandoned cropland classified as woody vegetation by 2017 were also the four sites entirely in forest biomes: Wisconsin, USA; Chongqing, China; Bosnia & Herzegovina; Vitebsk, Belarus / Smolensk, Russia), but it may simply be a result of insufficient time for woody biomass to develop, even in forest biomes. Land cover alone cannot confidently serve as a proxy for ecosystem recovery.

S1.4 The effect of varying abandonment definitions

A relatively short-term definition of abandonment might result in an overestimation of recultivation, by misclassifying long-term fallow cycles as periods of abandonment. In some cases, short-term abandonment may be better understood as cyclical fallow periods rather than true abandonment (33). Because the length of a typical fallow period may vary around the world, we tested multiple abandonment thresholds in order to test the sensitivity of our results to our choice of a five-year abandonment definition (which we selected following the FAO; 73). As our abandonment threshold increased in length, the mean abandonment duration across our sites increased accordingly, ranging between 8 years (no threshold) and 19 years (ten-year threshold; see Fig. S21). As expected, using a longer abandonment definition reduced the amount of cropland abandonment we detected, which is also shown in the area in the different colored age classes in Fig. 3.

The proportion of abandoned croplands that were recultivated by the end of the time series also responded to our abandonment threshold, with less recultivation for longer abandonment thresholds (Fig. S4). However, even at the longest abandonment definition (≥ 10 years), we still saw that between 11.91% and 30.13% of abandoned croplands were recultivated by the end of the time series (in Shaanxi/Shanxi, China and Volgograd, Russia respectively). We find that the mean area of abandoned croplands that get recultivated by the end of the time series declined from 38.05% with a five-year threshold to 30.95% with a seven-year threshold, and 22.58% with a ten-year threshold. This indicates that the abandonment and recultivation we observe is not merely a function of our five-year abandonment definition.

Finally, we also assessed how different thresholds of recultivation affected the mean duration of recultivation, finding a similar pattern to abandonment. When qualifying periods of abandonment were recultivated, we found that the mean length of recultivation increased as we increased the number of years that land needed to be continuously recultivated in order to be considered "recultivated" (Fig. S22).

S1.5 Comparing approaches to estimating abandonment: annual vs. two-timepoint estimates

Some studies estimate cropland abandonment by simply looking for differences between two cropland maps - in other words, by identifying areas where land cover is classified as "cultivated" in one year, but not in a later year (e.g., 1992 and 2015 in ref. 4). Such a method has the potential to overestimate abandonment by including short-term fallow periods and

discounting the potential for future recultivation. It also has the potential to underestimate abandonment by missing any new cultivation (and subsequent abandonment) that takes place between the two timepoints. To illustrate this point and understand the effect of using this simplified approach instead of our full annual time series, we estimated cropland abandonment by simply identifying areas that were classified as "cropland" in 1987 and classified as either "woody vegetation" or "herbaceous vegetation" in 2017 (excluding "non-vegetation").

Using this two-timepoint approach, we find only 5.00 Mha of "abandonment," a 17.49% underestimate compared to the 6.06 Mha of abandonment as of 2017 observed using our full annual time series. This "abandoned" area ranged from 45.07% less (Goiás, Brazil) to 46.38% more (Mato Grosso, Brazil) area abandoned at each site than the area identified using the full time series (Table S6). Furthermore, much of this "abandonment" consisted of croplands that had been abandoned for less than five years and therefore did not meet our definition of abandonment (ranging from 10.36% to 33.35% of area at all sites except Mato Grosso; see Table S6).

Not only did the two-timepoint method produce different area estimates, but it also identified geographically distinct areas of abandonment, with spatial agreement ranging from 28.5% (Goiás, Brazil) to 63.33% (Bosnia & Herzegovina) at our sites (Table S6). We measured spatial agreement using the Jaccard similarity index (*81*), a measure of overlap between two sets, defined as the proportion of shared elements, or the intersection divided by the union (Equation S1) (*81*):

$$J(a, b) = \frac{a \cap b}{a \cup b} \qquad (S1)$$

Section S2. Extended Methods

Our analysis builds on annual land cover maps for 1987-2017 developed by Yin et al. (*38*). The following section outlines our data processing and analytical methods in greater detail than was possible in the main text. We processed and analyzed our abandonment map data in RStudio version 2021.9.2.382 (*74*), using R version 4.1.2 (2021-11-01) (*75*), relying heavily on the `terra` (*76*), `data.table` (*77*), and `tidyverse` (*78*) packages. All area calculations were performed using the `terra` package's `cellSize()` function, which calculates the spherical area of each cell as defined by its four corners (*76*).

S2.1 Temporal filters

In order to address potential land-cover classification errors, we implemented a series of temporal filters designed to smooth trajectories by looking for short-term land-cover changes that are temporally unlikely. We applied five-year and eight-year moving-window filters that searched for short periods of land cover classifications that did not match those immediately before and after, and subsequently updated them to match the surrounding classifications. More specifically, the five-year filter searched for one year periods that did not match the two years immediately before and after the central year (e.g., patterns of `11011`, where `1` represents non-cropland and `0` represents cropland, or vice versa), and our eight-year filter searched for two year periods that did not match the three years before and after (i.e., `11100111`). Both filters then updated the central classifications to match the classes on either end. We applied these filters to

the raw land cover maps for each land cover class sequentially (cropland, herbaceous vegetation, woody vegetation, and non-vegetation), prior the identification of abandoned cropland.

S2.2 Classifying abandonment

We only included periods of abandonment that verifiably followed agricultural activity during our time series. Accordingly, pixels that were consistently cropland or consistently non-cropland (i.e., herbaceous or woody vegetation) classes throughout time were excluded. This also meant that we excluded periods of non-cropland classification that began in the first year of the time series, because of a lack of information on whether this non-cropland had been previously cultivated. Accordingly, if pixels were initially non-cropland, then changed to cropland and were subsequently abandoned, we only counted these last periods as abandonment.

To illustrate this, consider the following time series read left to right, which represents twenty years beginning at the start of our time series (where `1` represents non-cropland and `0` represents cropland):

```
'87 '88 '89 '90 '91 '92 '93 '94 '95 '96 '97 '98 '99 '00 '01 '02 '03 '04 '05 '06
 1   1   1   1   1   1   1   0   0   0   0   1   1   1   1   1   1   1   1   1
```

This represents seven years of non-cropland to start the time series, followed by four years of cropland cultivation, followed by nine years of non-cropland. Though this pixel experienced two periods of non-cropland classification of five or more years (from 1987 through 1993, and from 1998 through 2006), we only include the second, nine-year period (1998 through 2006), because it clearly followed cropland classification.

As noted in the main text, pixels that transitioned from cropland to the non-vegetation land cover class were not considered "abandoned," and therefore we excluded all non-vegetation pixels from our entire analysis. These pixels accounted for <10% of total site area at all sites except Shaanxi/Shanxi, China (12.7%) and Iraq (52.8%), and remained stable or declined over time at all eleven sites (see Fig. S20).

S2.3 Estimating soil organic carbon accumulation

We derived mean soil organic carbon (SOC) accumulation rates from the Soils Revealed database (39). Soils Revealed contains multiple scenarios of SOC accumulation under different land-use change outcomes, including one that estimates the SOC that could accumulate in agricultural lands (cropland and pastures) following a full return to native vegetation. This scenario estimates SOC stocks after 20 years and 80 years of natural regeneration. In order to translate this into an annual rate of soil organic carbon accumulation, we first extracted SOC stock values for only those pixels that transitioned from cropland to native vegetation (after identifying cropland pixels with the IPCC land cover map used in development of the database), and calculated the mean stock at 20 and 80 years at each site, to allow for consistent application to our finer resolution cropland map, which included some cropland areas not mapped by the coarser IPCC land cover map. First, we calculated an annual SOC accumulation rate to be applied during the first 20 years of regeneration by simply dividing the 20-year stock value by 20 (Fig. S13). To calculate an annual SOC accumulation rate to apply to years 21 through 80, we divided the difference between the 80-year and 20-year SOC stock by 60 (Fig. S14).

S2.4 Modeling abandonment recultivation as a "decay" process

Our mean abandonment duration metric tells us about the general persistence of abandoned croplands throughout the time series. However, this duration value is limited by the time series length, and does not account for when the majority of the abandonment took place at a site, nor whether a period of abandonment ends as a result of recultivation or the end of the time series. As a result, the mean abandonment duration does not tell us how long to expect a piece of land to remain abandoned, nor how abandonment length varies through time. To address this constraint, we track the trajectory of each abandoned pixel through time following its initial abandonment, grouping pixels abandoned in a given year into "cohorts." Decay trajectories derived from this approach provide information about how long it takes for land to be recultivated, complementing the mean abandonment length and providing a more nuanced story about how long to expect abandonment to last.

For example, a site may have a relatively short mean length of abandonment (e.g., Shaanxi/Shanxi, China, with a mean abandonment length of 12.93 years; Fig. 4, Table S1), but also have a gradual decay rate, indicating that land is like to stay abandoned for a relatively longer amount of time than observed during the time window of our time series. This may result from more abandonment occurring towards the end of the time series; this land simply does not have as long to age and shows up as younger in our data, regardless of how long it may last in the future. Looking at abandonment decay rates for each cohort individually allows us to produce mean decay trajectories for each site in a way that accounts for when a piece of land was first abandoned during the time series (i.e., giving us a sense of how long to expect a given piece of land to remain abandoned, even into the future).

S2.4.1 Model selection and diagnostics

We fit a linear model using the `lm()` function in R's core statistics package `stats`, predicting the proportion of abandoned cropland in each cohort remaining abandoned as a function of time since initial abandonment at each site. The proportion of abandoned cropland remaining abandoned is measured relative to the area abandoned five years following the year of initial abandonment, as dictated by our five-year abandonment definition.

We tested a range of model specifications, including linear and log transformations of both *proportion* and *time*. Due to a linear relationship between model residuals and time when including only one term for *time*, we also tested models containing multiple *time* predictor terms, including both log and linear terms.

We chose a model with the specifications shown in Equation 1 and reproduced here in Equation S2. For cohorts of abandonment initially abandoned in years $y = 1988,\ldots,2013$, we estimate the proportion p of each cohort y at site z remaining abandoned as a function of time t (i.e., based on the number of years after initial abandonment).

$$p_{yz} = 1 + \beta_{yz,1}\log(t+1) + \beta_{yz,2}t \qquad (S2)$$

Where $\beta_{yz,1}$ represents the regression coefficient on the log term of time t for cohort y at site z, and $\beta_{yz,2}$ represents the regression coefficient on the linear term of time t for cohort y at site z. We allow for *cohort* and *site* fixed effects, fitting unique coefficients for each cohort at each site.

We ran a single pooled model using data across all 11 sites, using the following function call: `stats::lm(formula = I(proportion - 1) ~ 0 + log(time + 1):cohort:site + I(time):cohort:site)`. The observations and fitted values for each cohort from our pooled linear model are shown in Fig. 6.

Model selection was performed based on Akaike Information Criterion (AIC) values (Fig. S24), selecting the model with the lowest (i.e., more negative) AIC value. We confirmed that linear model assumptions were not violated through visual inspection of both residuals vs. fitted plots and Q-Q plots (Fig. S28).

S2.4.2 Comparing across cohorts using common endpoints

As noted in the main text, we calculate mean decay trajectories at each site for a range of common endpoints (7-29 years; see Fig. S17). This method of parameterizing our pooled linear model for subsets of our data according to common endpoints was developed in order to facilitate fair comparisons across cohorts, specifically by ensuring that mean coefficient values would be calculated after restricting each cohort to the same number of observations in the calculation of coefficients to be averaged. In order to calculate the mean decay trajectory for a given site at a given endpoint (as shown by the red lines in Figs. S26-S27), we took the mean of the log coefficients ($\beta_{\bar{y}z,1}$) and the mean of the linear coefficients ($\beta_{\bar{y}z,2}$) respectively across all cohorts y at each site z that met the threshold for each given endpoint. We then used these mean coefficient values ($\beta_{\bar{y}z,1}$ and $\beta_{\bar{y}z,2}$) to define a new function describing the mean recultivation (or decay) trajectory for each site at each endpoint, using the same form as Equation (S2).

S2.5 Change in recultivation rates over time

We examined the rate of change of recultivation rates by calculating the half-life, defined as the time required for half (50%) of a given cohort of abandoned cropland to be recultivated at a given site, and parameterizing a simple linear model on these half-life values as a function of time, using the `stats::lm()` function in R's core statistics package `stats`. This resulted in $n = 26$ half-life values (one for each cohort) at each of our 11 sites. We estimate the half-life, $t_{half,z}$, as a function of the year of initial abandonment ($yearabn_z$), at each site z, as shown in Equation (S3).

$$t_{half,z} = \beta_{0,z} + \beta_{1,z} yearabn_z \quad (S3)$$

Where $\beta_{1,z}$ represents the regression slope on the year abandoned (cohort) for site z ($yearabn_z$), and $\beta_{0,z}$ represents the intercept. This corresponds to a `stats::lm()` call of `lm(formula = t_half ~ year_abandoned)`, run for each site individually. Results are shown in Fig. S18. We confirmed that model assumptions were met through visual inspection of residuals vs. fitted plots and Q-Q plots (Fig. S29).

Section S3. Supplementary Figures
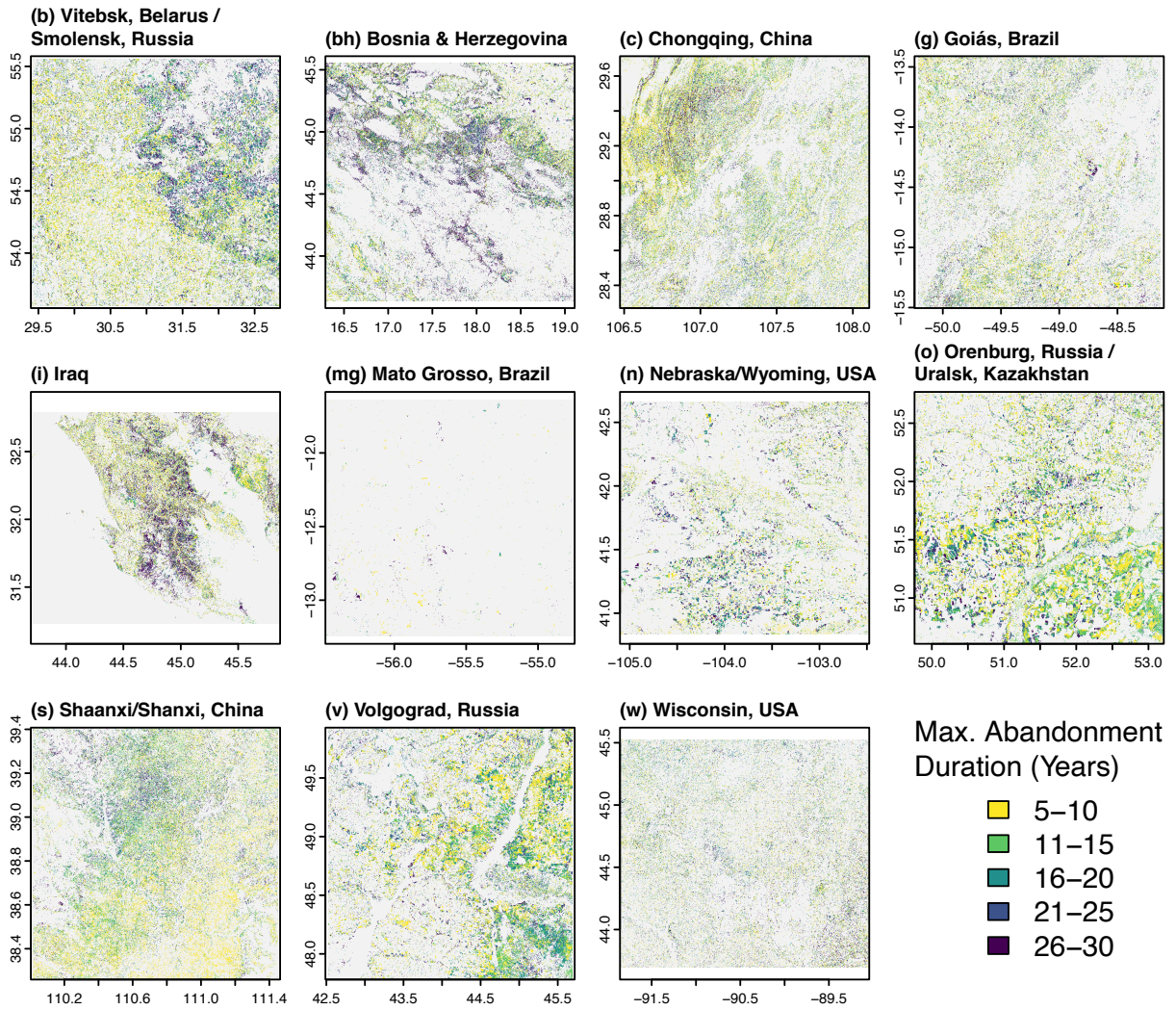
Fig. S1.

Maximum duration of cropland abandonment (in years) observed at each pixel between 1987 and 2017 in our eleven study sites. X axes show degrees longitude relative to the prime meridian (negative indicating west and positive indicating east), and y axes show degrees latitude relative to equator (negative indicating south and positive indicating north). This serves as a companion to maps of the abandonment duration as of 2017 shown in Fig. 2. Site locations are shown in Fig. 1.
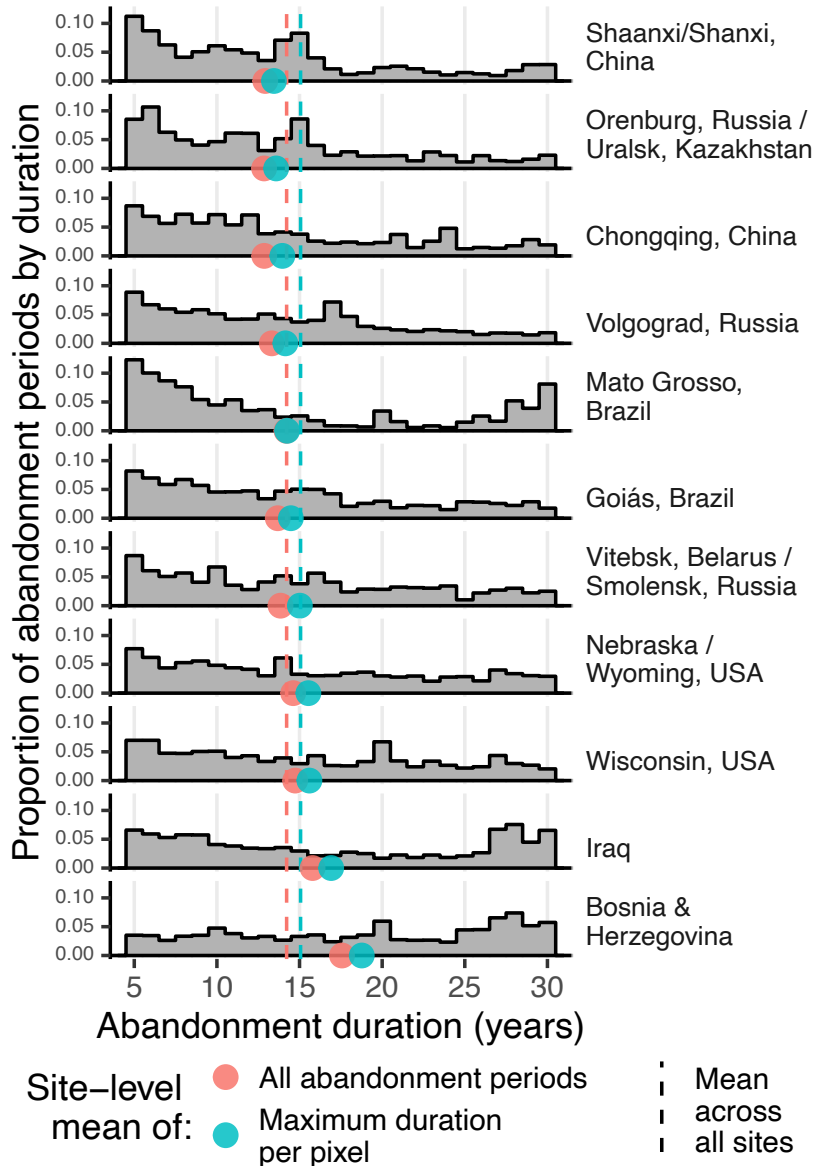
Fig. S2.

The distribution of the maximum abandonment duration (in years) for each pixel at each site from 1987 to 2017. The y-scale shows the proportion of pixels with maximum duration values of a given duration at each site. As previously noted, abandonment and recultivation can occur multiple times at a single pixel during our time series, and this figure serves as a companion to the distribution of all abandonment periods shown in Fig. 4. Site-level mean duration values are shown in the red and blue dots, corresponding to mean values calculated across all periods of abandonment (in red, including multiple periods per pixel) and mean values calculated across only the maximum duration of abandonment at each pixel (in blue). The vertical dashed lines represent the mean of these site-level mean duration values, for all abandonment periods (red) and only the maximum duration at each pixel (blue), respectively.
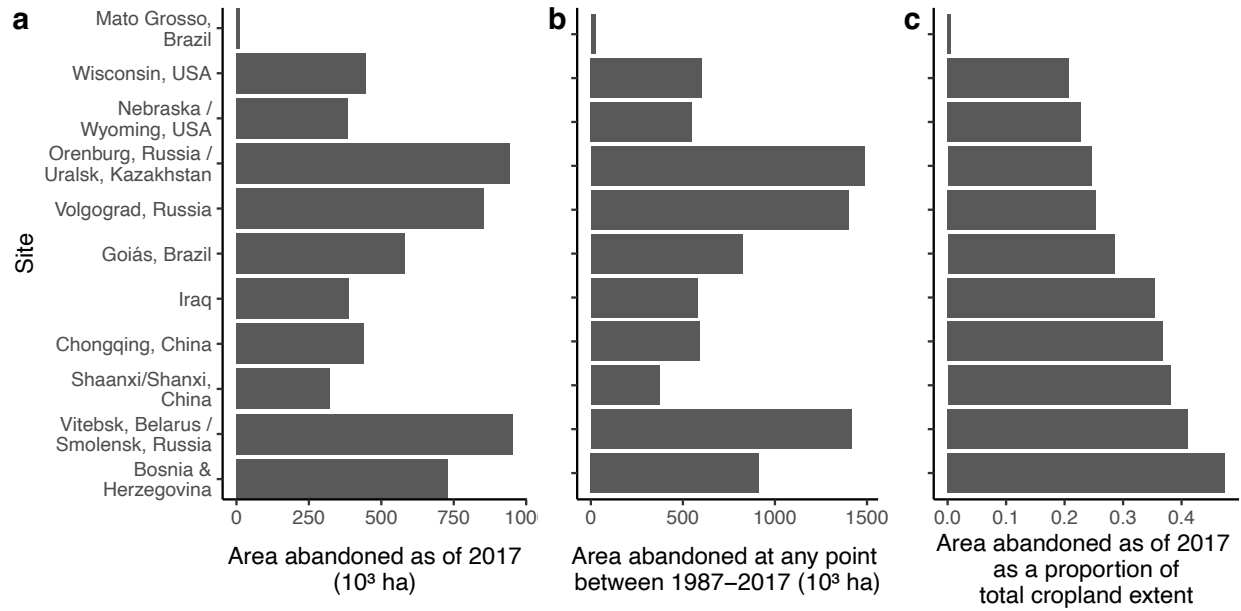
Fig. S3.

Abandonment area as of 2017, across three categories: a) area of abandonment observed as of 2017, b) area of all croplands abandoned at least once between 1987-2017 (i.e., the potential area abandoned by 2017, assuming no recultivation), c) observed area abandoned as of 2017 as a proportion of the total cropland extent (i.e., the area of all lands that were cultivated at some point during the time series). Note that sites are shown in ascending order of area abandoned as of 2017 as a proportion of total cropland extent.
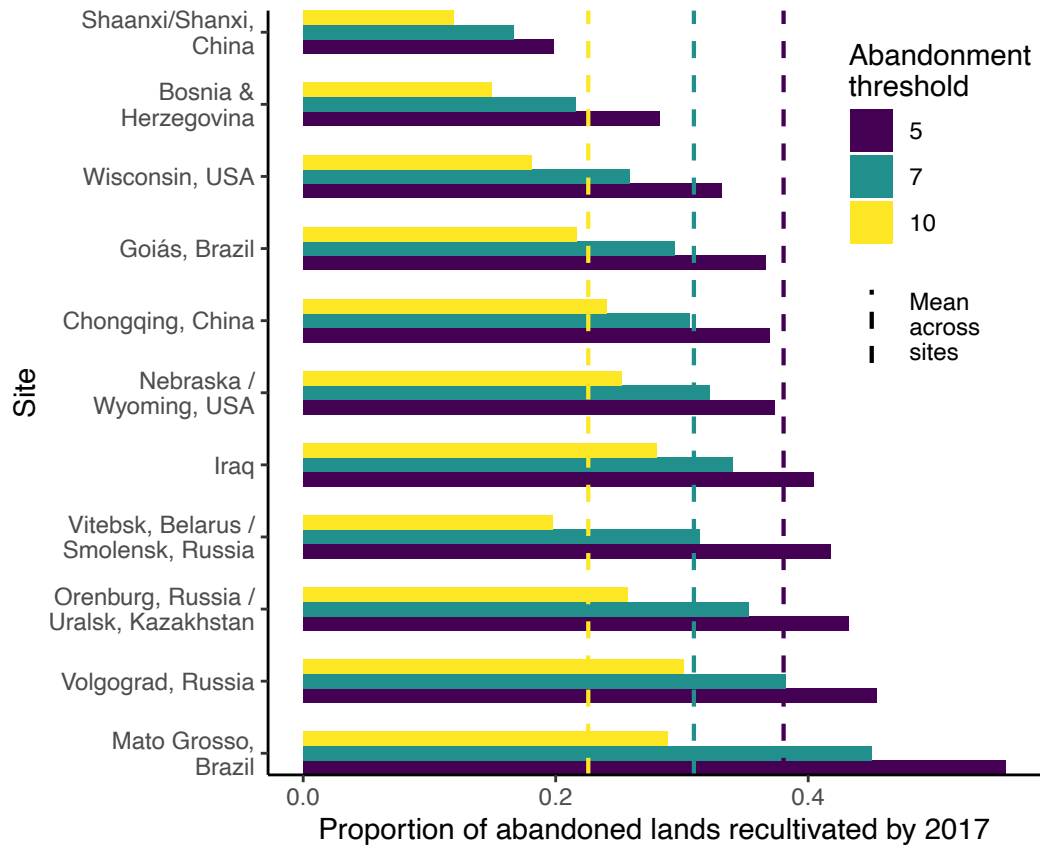
Fig. S4.

Recultivation rates shown for various abandonment thresholds.
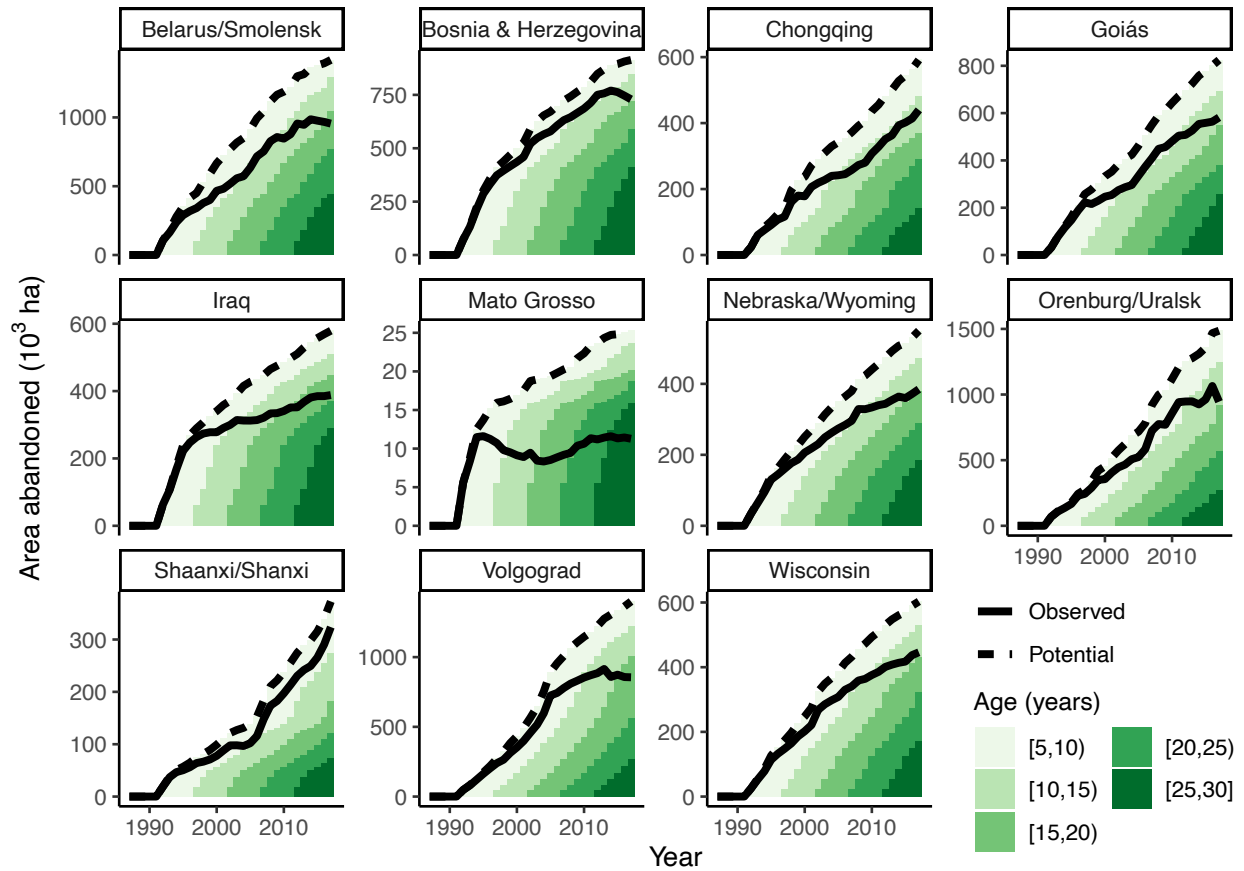
Fig. S5.

Potential area abandoned over time, assuming no recultivation took place, shown according to age class (in years). Cumulative potential area abandoned at each site is shown as the dashed black line, and the cumulative observed area abandoned is shown for comparison as the solid black line. This figure serves as a companion to Fig. 3.
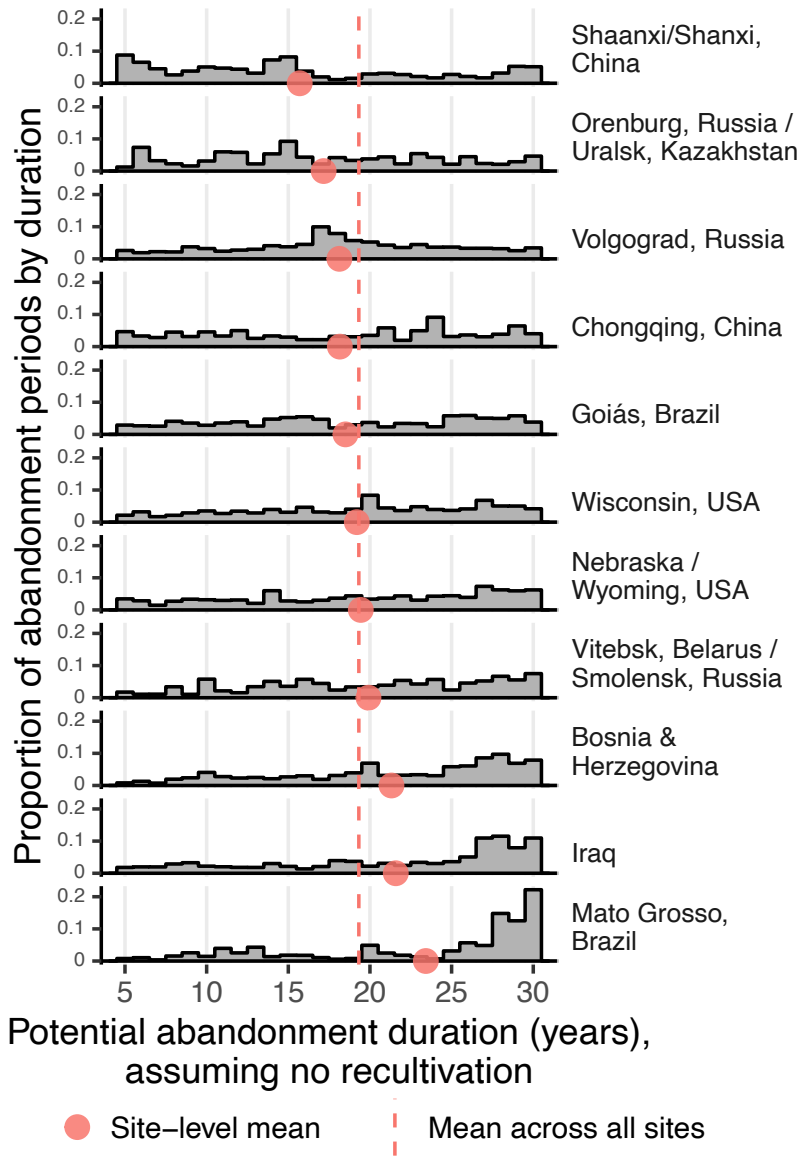
Fig. S6.

The distribution of potential abandonment duration (in years) for all periods of abandonment from 1987 to 2017, assuming no recultivation occurred following abandonment that met our five-year threshold. The y-scale shows the proportion of potential abandonment periods of a given duration at each site. The red points represent the potential mean abandonment duration (in years) at each site, and the red vertical dashed line represents the mean of these site-level mean duration values across all sites. This serves as a companion to the distribution of observed abandonment periods in Fig. 4.
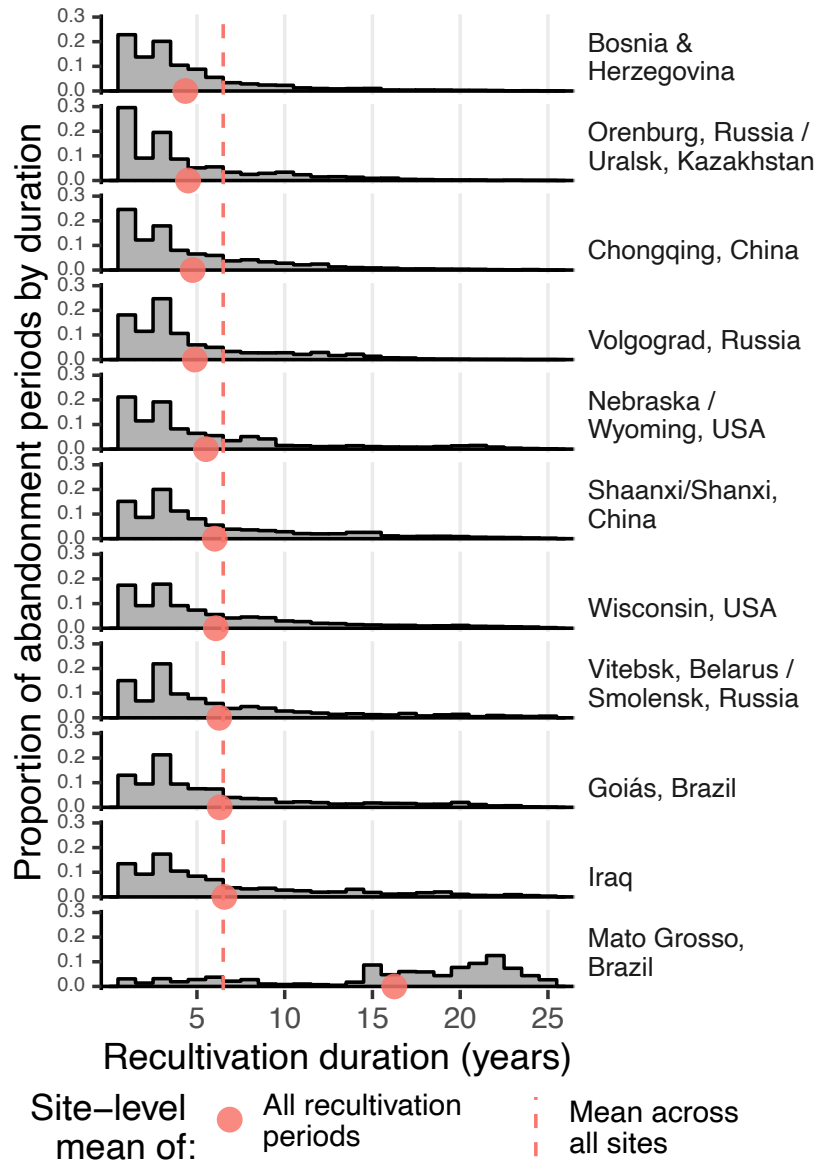
Fig. S7.

The distribution of duration of recultivation periods that took place after qualifying periods of abandonment. Recultivation (in which abandoned croplands were reclassified as active cropland for one or more years) could take place at any point in or after 1993 (as a result of our five-year abandonment threshold). Note that we included all periods of recultivation, regardless of length, given that recultivation of even one year is biologically relevant to the process of secondary succession. The y-scale shows the proportion of pixels with recultivation periods of a given duration at each site. As previously noted, abandonment and recultivation can occur multiple times at a single pixel during our time series, and this figure serves as a companion to the distribution of all abandonment periods shown in Fig. 4. Site-level mean duration values are shown as red dots, corresponding to mean values calculated across all periods of recultivation (including the possibility of multiple periods per pixel). The vertical dashed lines represent the mean of these site-level mean duration values, for all recultivation periods.
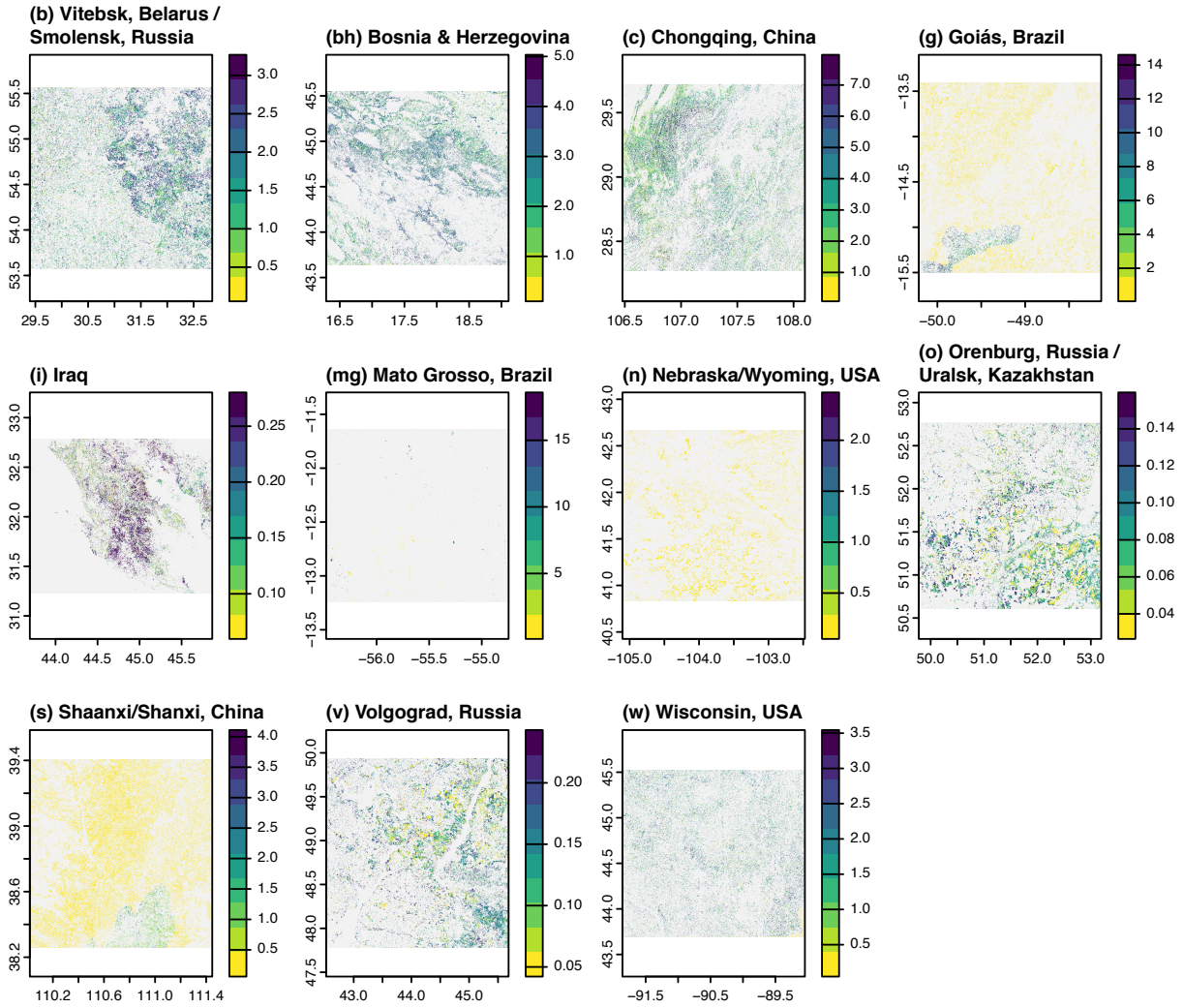
Fig. S8.

Cumulative carbon accumulation in abandoned croplands as of 2017, in terms of Mg C per pixel (30-m resolution). This cumulative value incorporates both carbon accumulated in forested biomes (including aboveground biomass, belowground biomass, and soil organic carbon; *31*) and soil organic carbon accumulated in non-forested biomes (*39*). Forested biomes were delineated using Ecoregions2017 (*79*). X axes show degrees longitude relative to the prime meridian (negative indicating west and positive indicating east), and y axes show degrees latitude relative to equator (negative indicating south and positive indicating north).
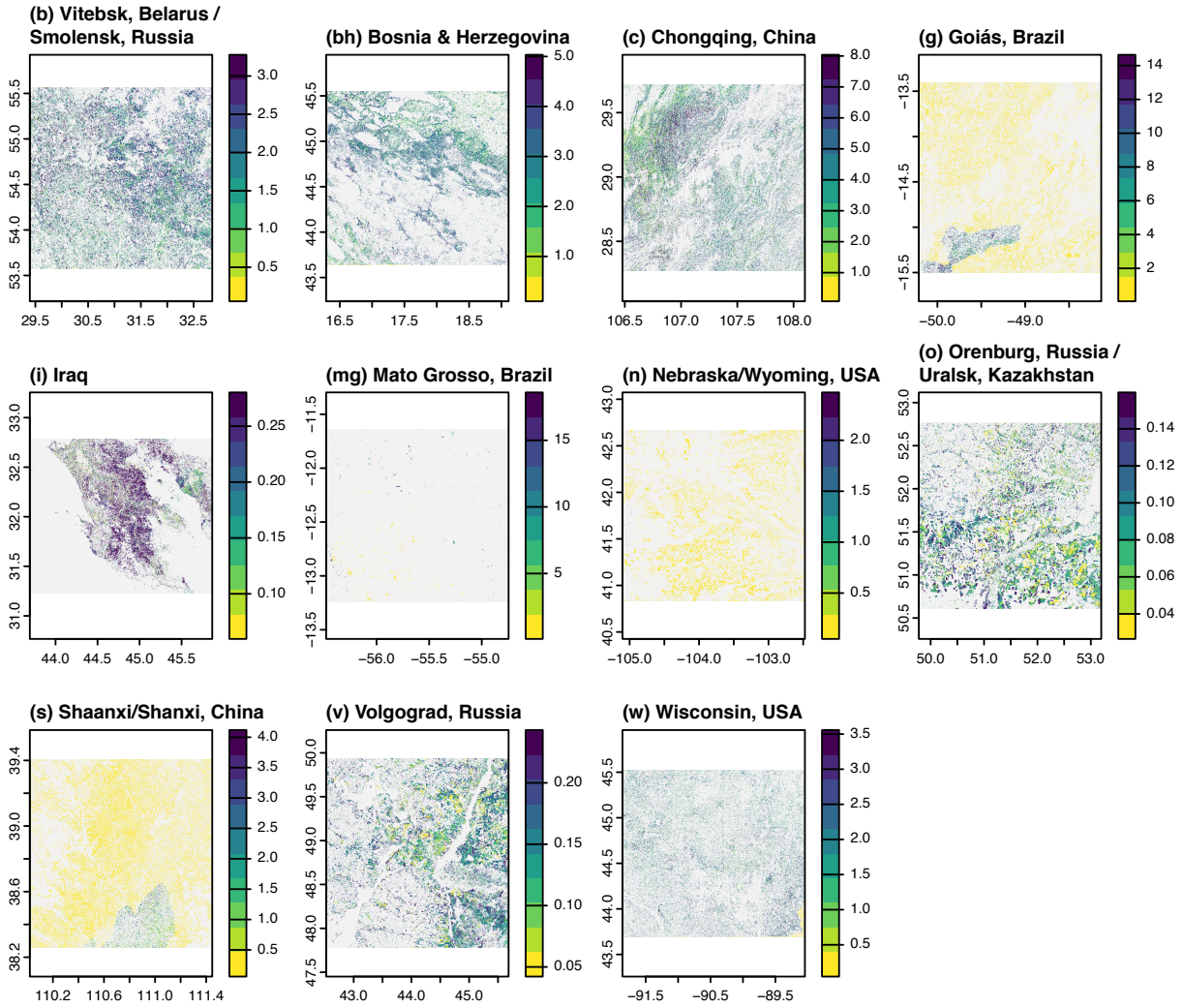
Fig. S9.

Potential carbon accumulation in abandoned croplands as of 2017, assuming no recultivation of abandoned croplands, in terms of Mg C per pixel (30-m resolution). Calculated using identical carbon accumulation rates as Fig. S8, but assuming no recultivation. X axes show degrees longitude relative to the prime meridian (negative indicating west and positive indicating east), and y axes show degrees latitude relative to equator (negative indicating south and positive indicating north).
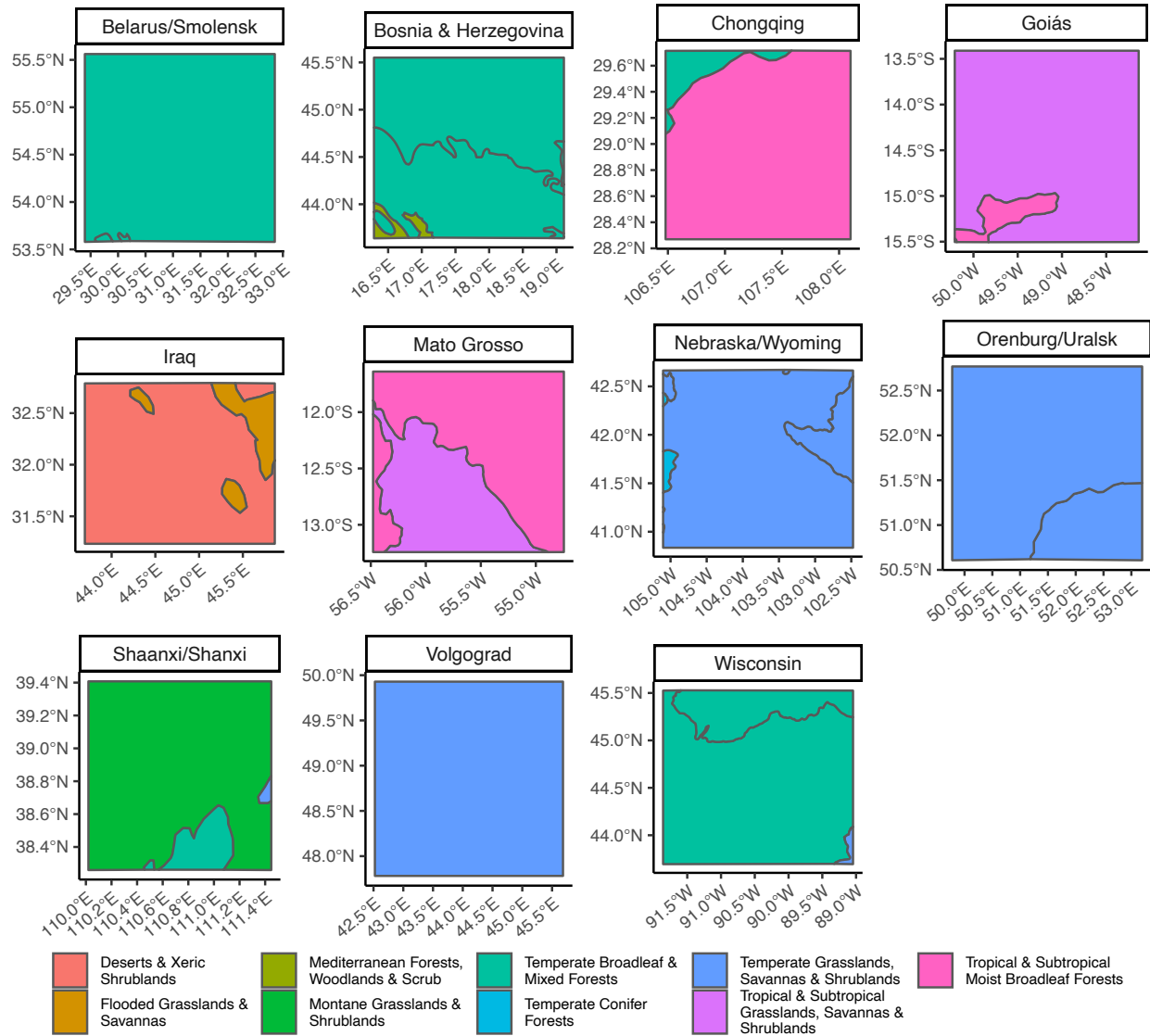
Fig. S10.

Biomes at each site, derived from Ecoregions2017 (*79*).
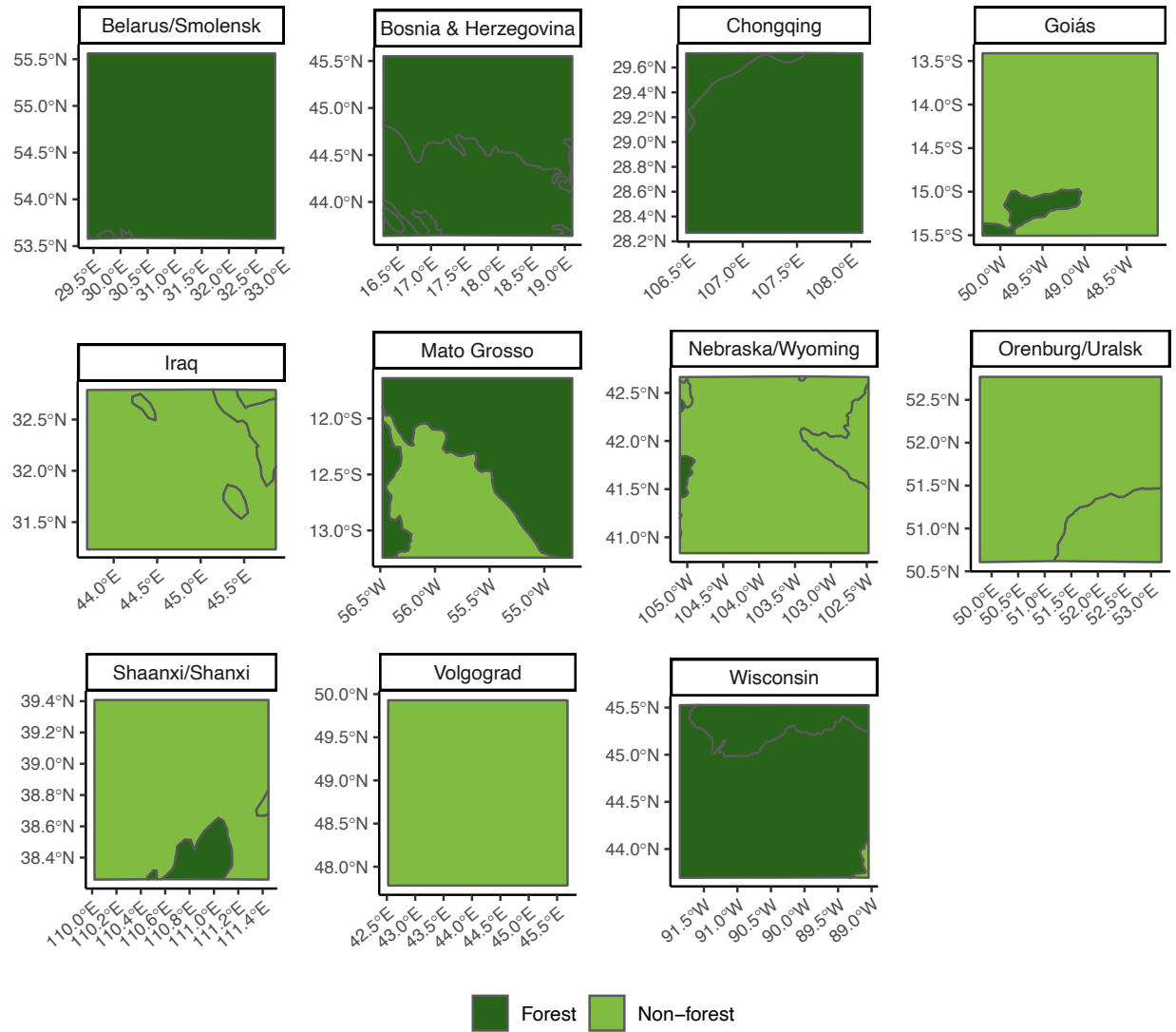
Fig. S11.

Biomes at each site, separated into forest and non-forest, derived from Ecoregions2017 (*79*).
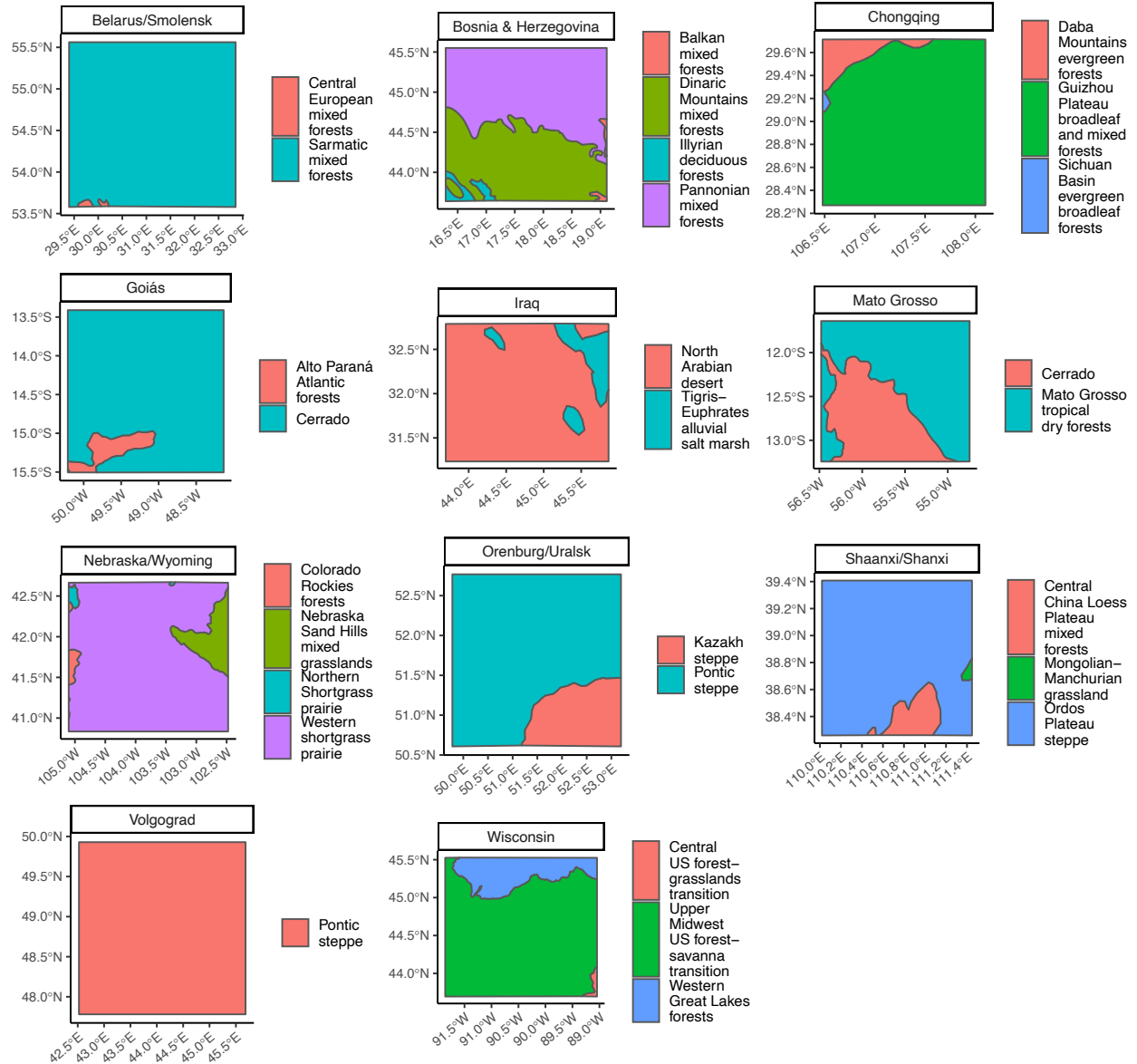
Fig. S12.

Ecoregions at each site, from Ecoregions2017 (*79*).
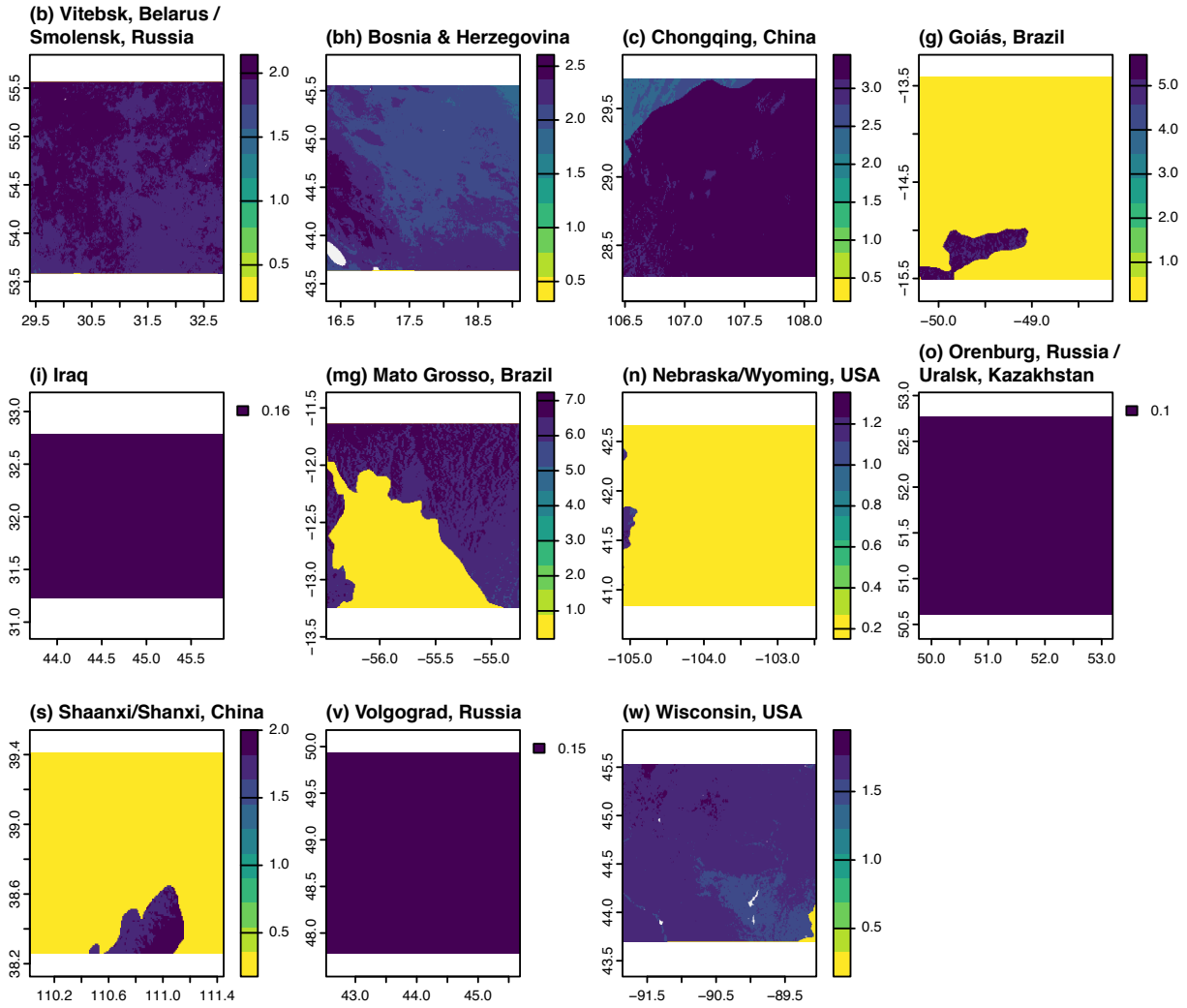
Fig. S13.

Annual carbon sequestration rates for the first 20 years of secondary succession, in terms of Mg C per hectare. Forest carbon sequestration rates are drawn from (*31*), and include aboveground biomass, belowground biomass, and soil organic carbon, and apply for the first 30 years of secondary succession. Soil organic carbon sequestration rates in non-forest biomes are drawn from (*39*), and apply for the first 20 years of secondary succession. Forested biomes were delineated using Ecoregions2017 (*79*). See Fig. S11. X axes show degrees longitude relative to the prime meridian (negative indicating west and positive indicating east), and y axes show degrees latitude relative to equator (negative indicating south and positive indicating north).
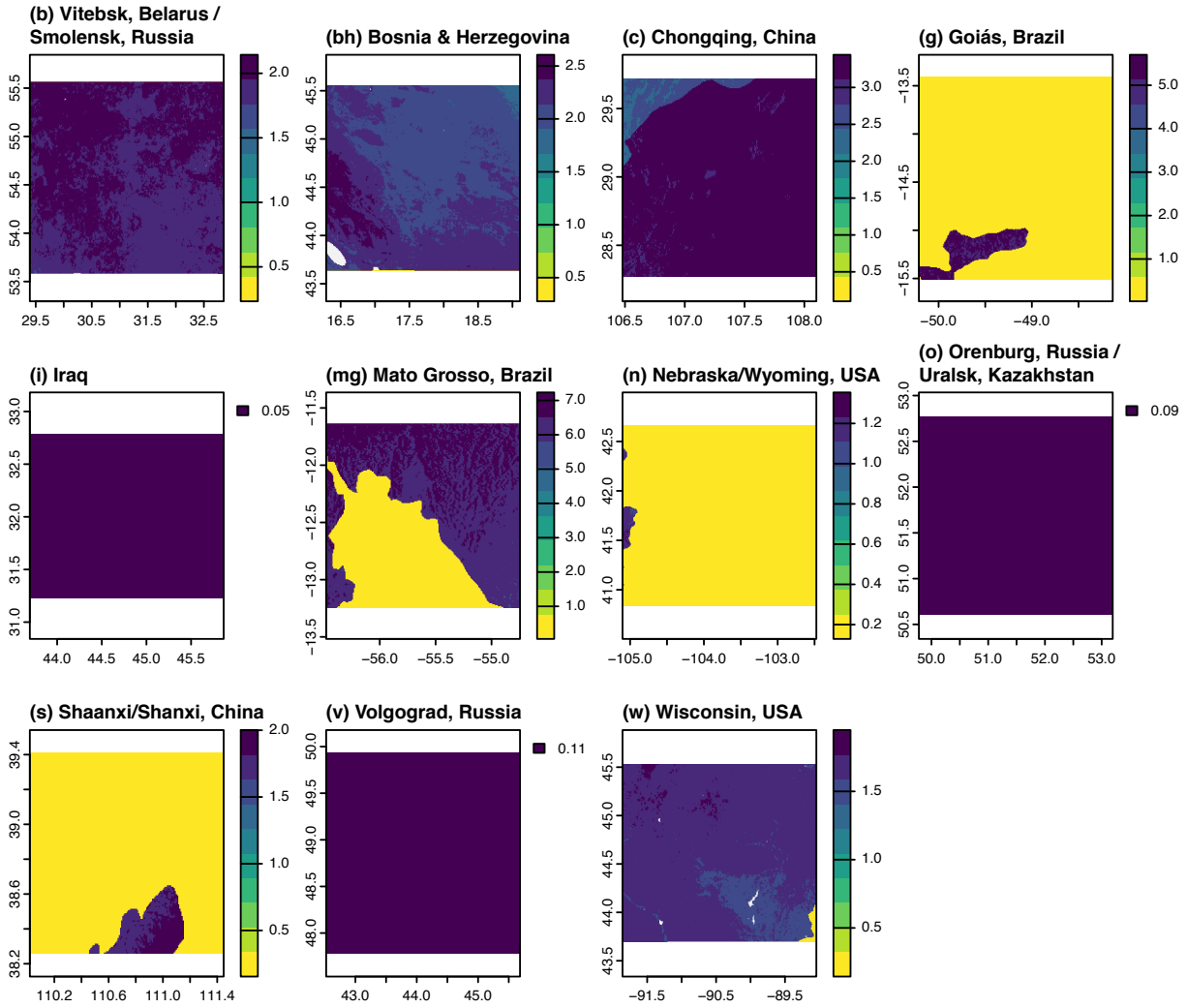
Fig. S14.

Annual carbon sequestration rates for the third decade of secondary succession (years 21 through 30), in terms of Mg C per hectare. Forest carbon sequestration rates are drawn from (*31*), and include aboveground biomass, belowground biomass, and soil organic carbon, and apply for the first 30 years of secondary succession. Soil organic carbon sequestration rates in non-forest biomes are drawn from (*39*), and are calculated from estimated "steady state" values after 80 years of succession. Forested biomes were delineated using Ecoregions2017 (*79*). See Fig. S11. X axes show degrees longitude relative to the prime meridian (negative indicating west and positive indicating east), and y axes show degrees latitude relative to equator (negative indicating south and positive indicating north).
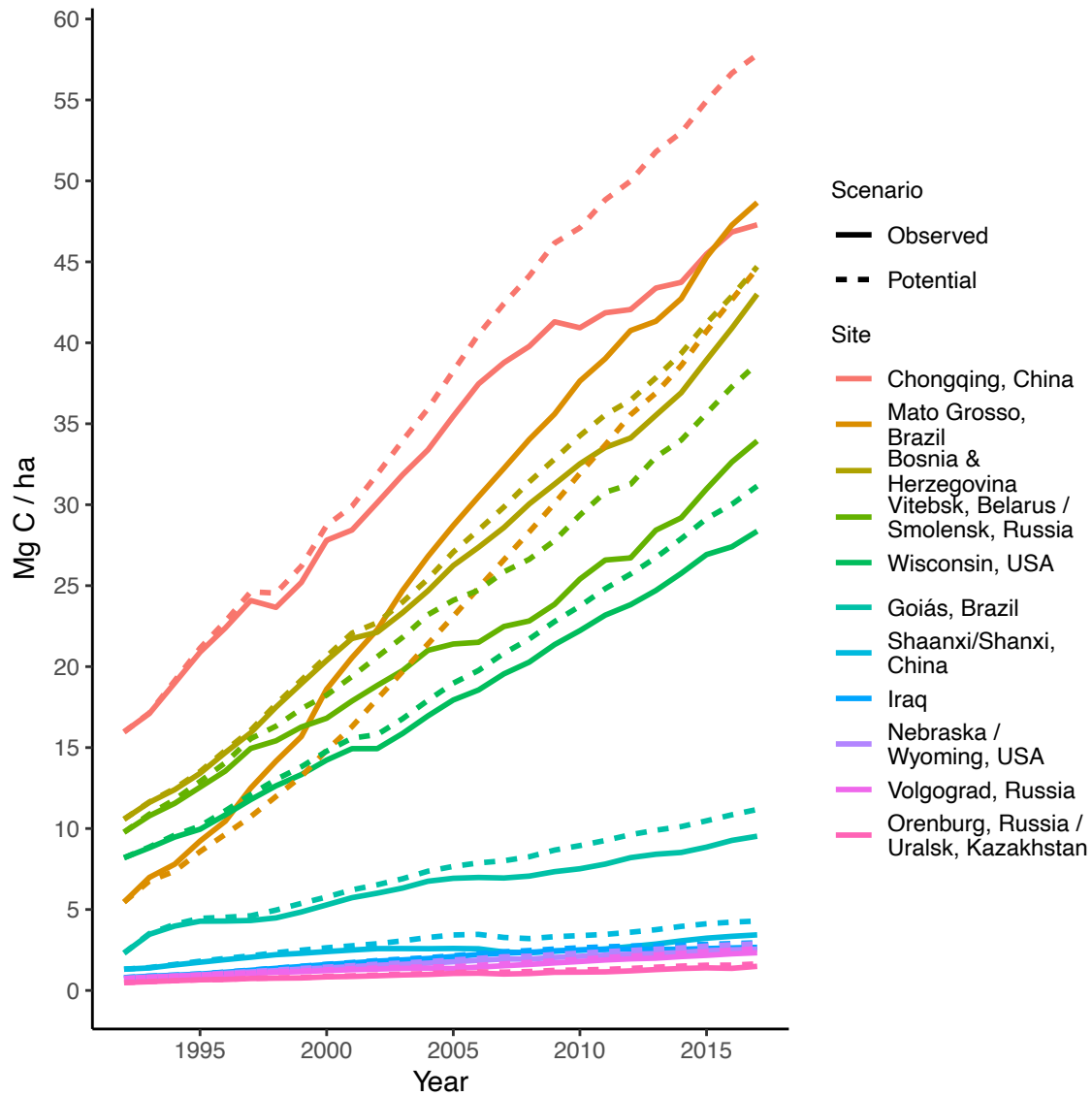
Fig. S15.

Total carbon accumulation per hectare over time.
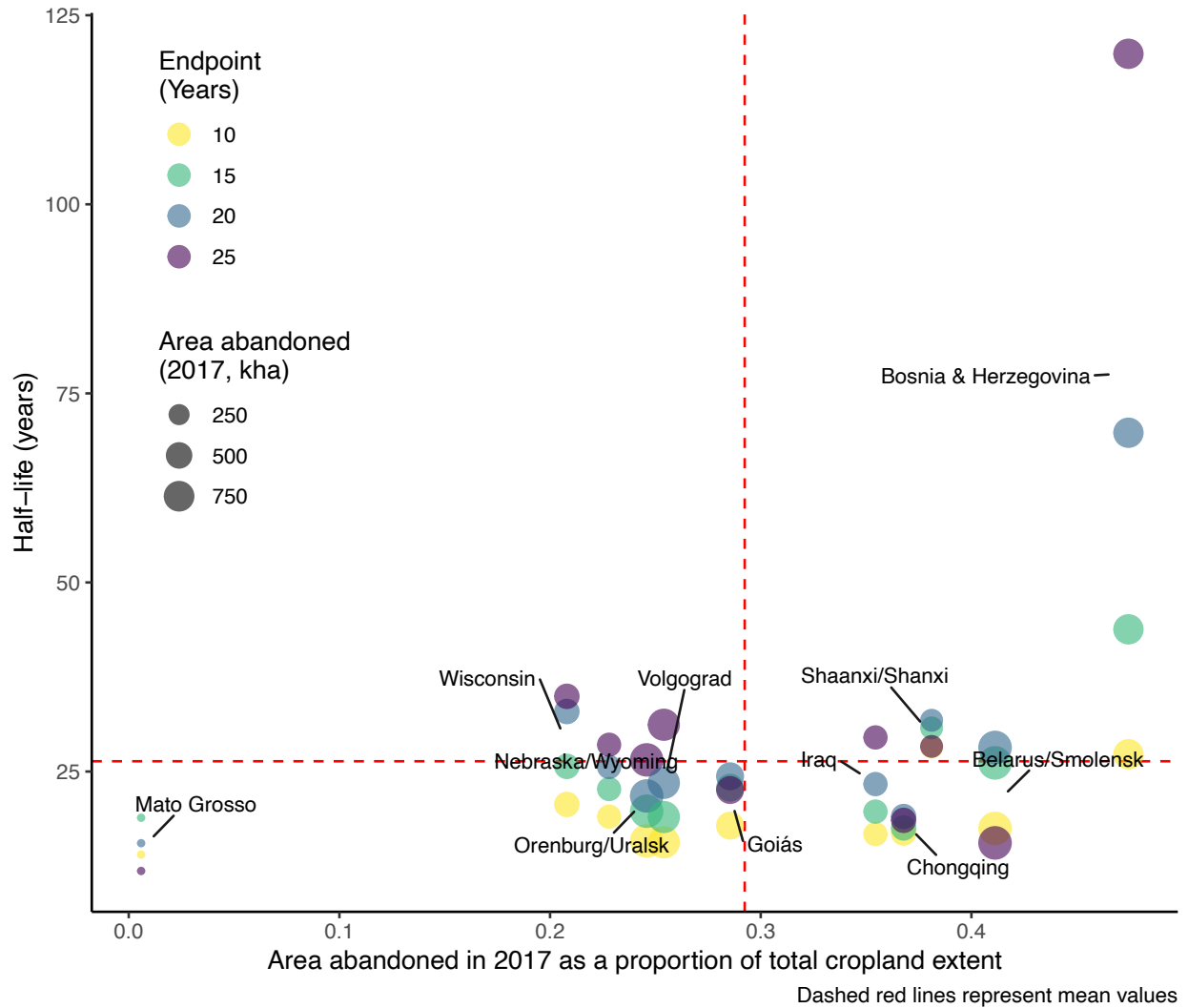
Fig. S16.

Abandonment decay as a function of extent of abandonment at each site. Abandonment decay is shown on the y-axis, as half-lives for endpoints of 10, 15, 20, and 25 years (represented by yellow to purple colors). Abandonment extent is shown on the x-axis as the area abandoned in 2017 as a proportion of the total cropland extent at each site. The absolute area abandoned as of 2017 is shown by the size of the points for each site. The red dashed lines represent the mean values for each axis.
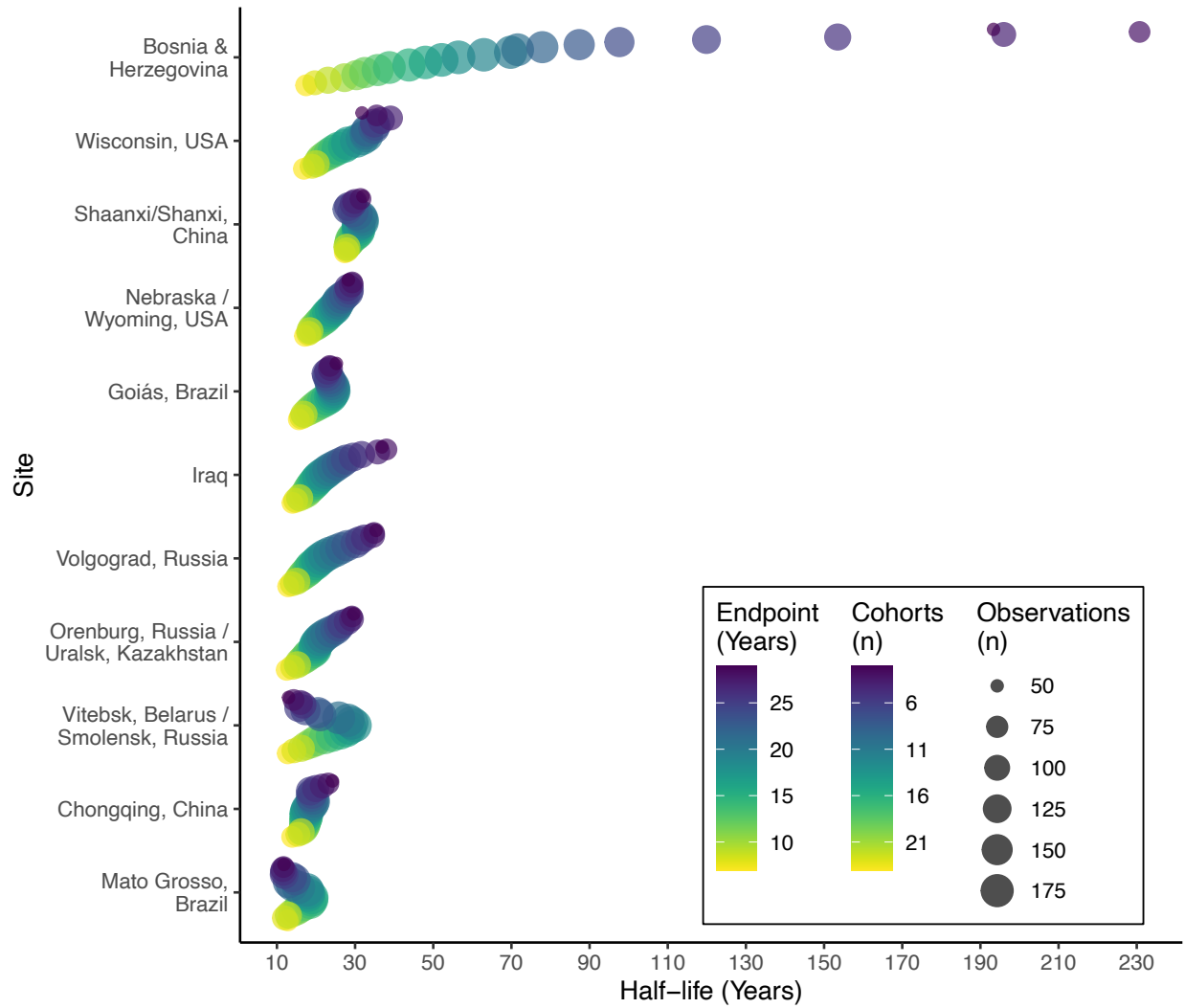
Fig. S17.

Mean half-lives of abandoned croplands at each site, calculated across our full range of common endpoints (7 to 29 years). See Materials and Methods for a description of our common endpoint modeling approach. These half-lives are calculated for mean site trajectories calculated across model runs at a specific common endpoint (e.g., 15 years), in order to make fair comparisons across cohorts with varying numbers of observations. This serves as a full companion to Fig. 7.
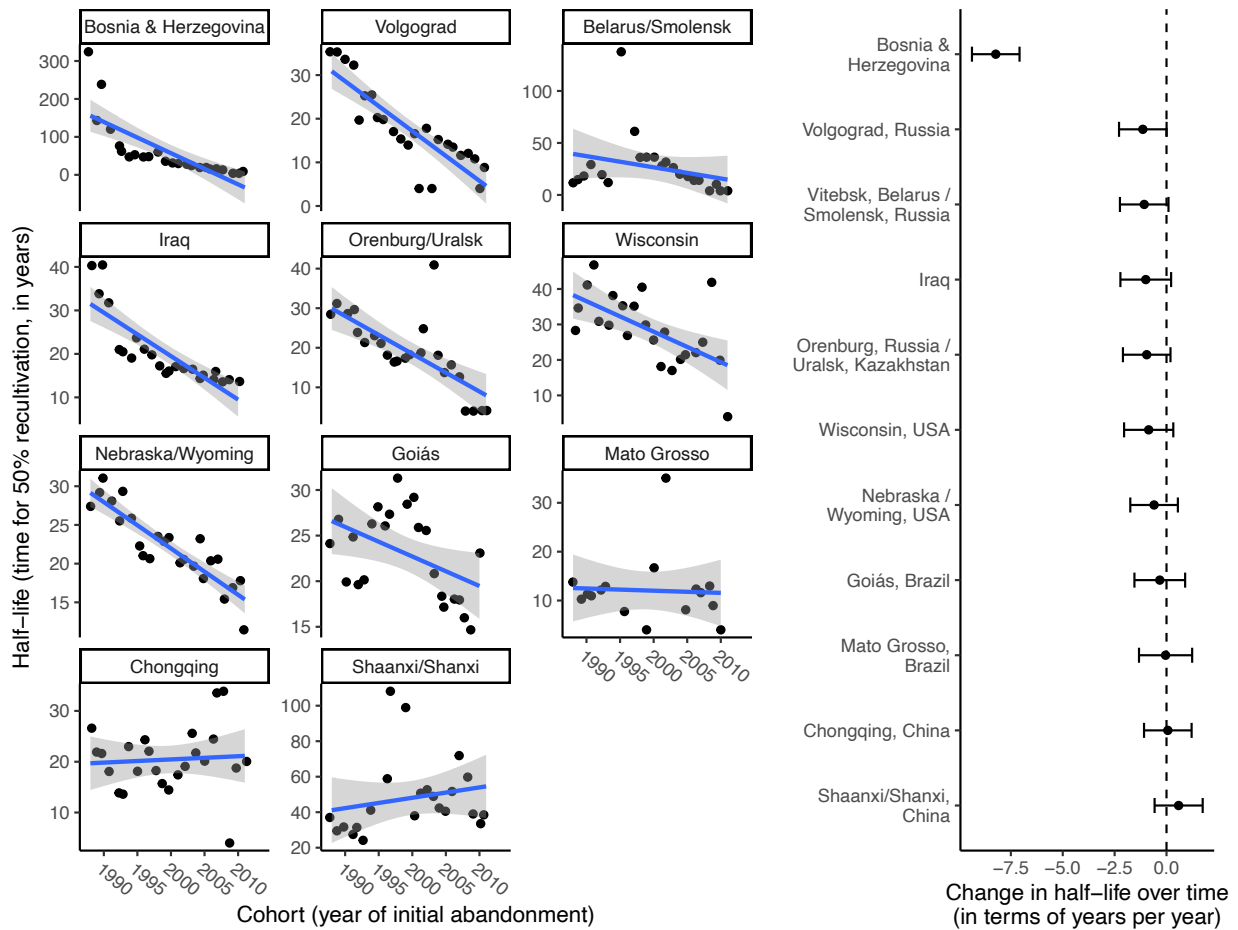
Fig. S18.

The rate of change of decay rates (measured as the half-life, or the time required for 50% of each cohort to be recultivated) at each site over the course of the time series. Individual site trends are shown in panel a. Solid lines show simple linear regressions, the slopes of which are shown in panel b. Gray bands around the linear trends in panel a and the error bars on slope estimates in panel b both represent 95% confidence intervals. These models are described by Eq. (S3). Model diagnostic plots are shown in Fig. S29.
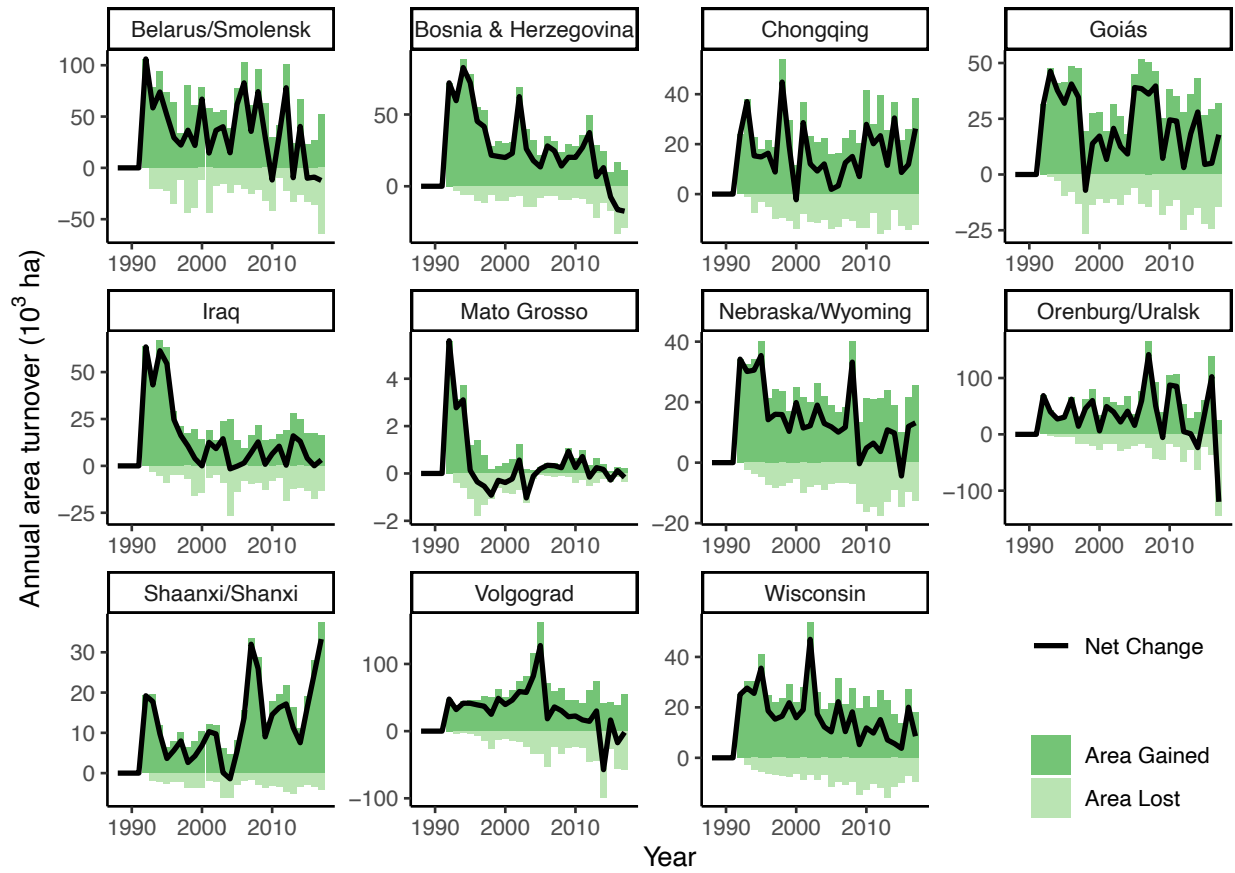
Fig. S19.

Annual turnover of abandoned croplands at each site, showing the annual gain (dark green) and annual loss (i.e., recultivation, light green) and net change (black line) of abandoned croplands.
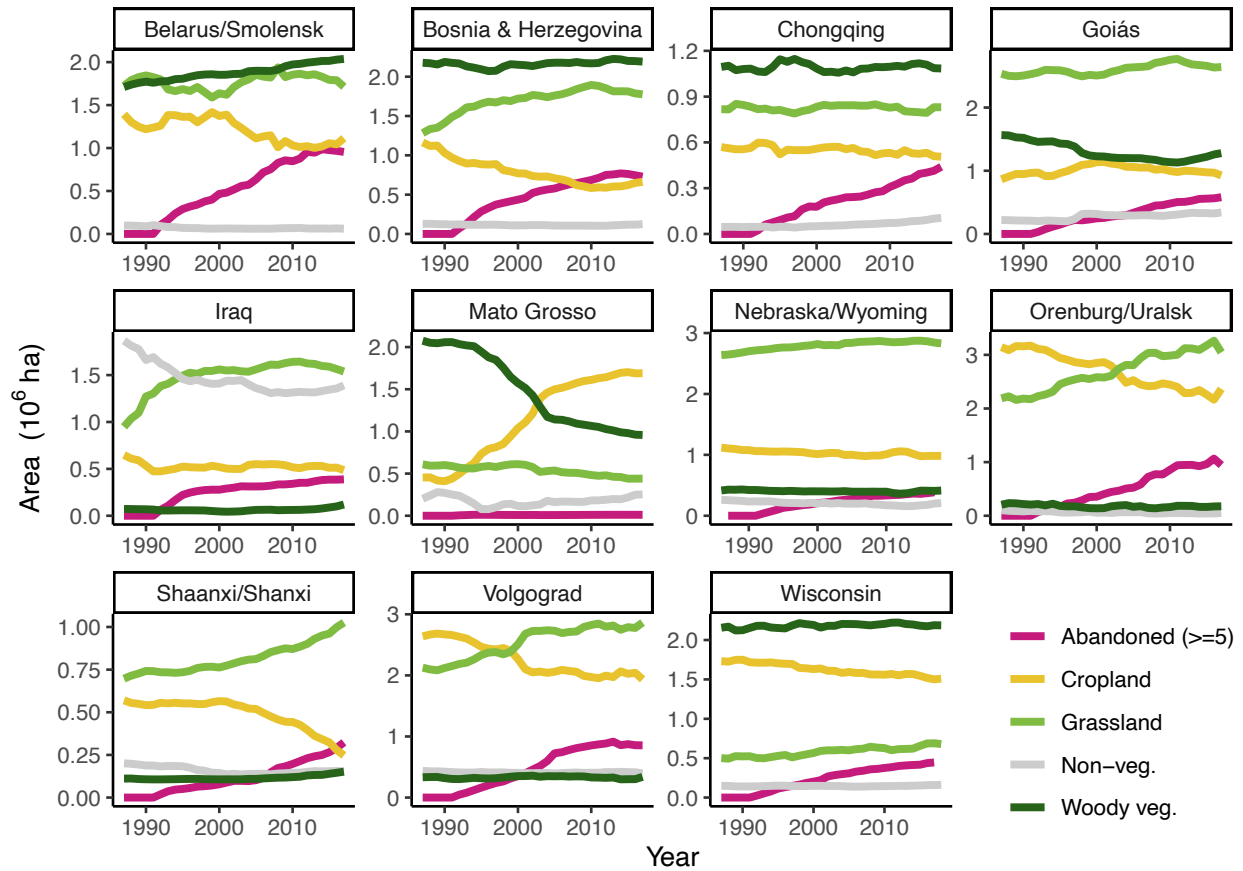
Fig. S20.

Area in each land cover class at each site through time. Mapped land cover classes are cropland, grassland, woody vegetation, and non-vegetation. Note that the area abandoned (for at least 5 years, shown in pink) consists of increases in grassland and woody vegetation that took place on former croplands. Therefore, these three classes are not mutually exclusive.
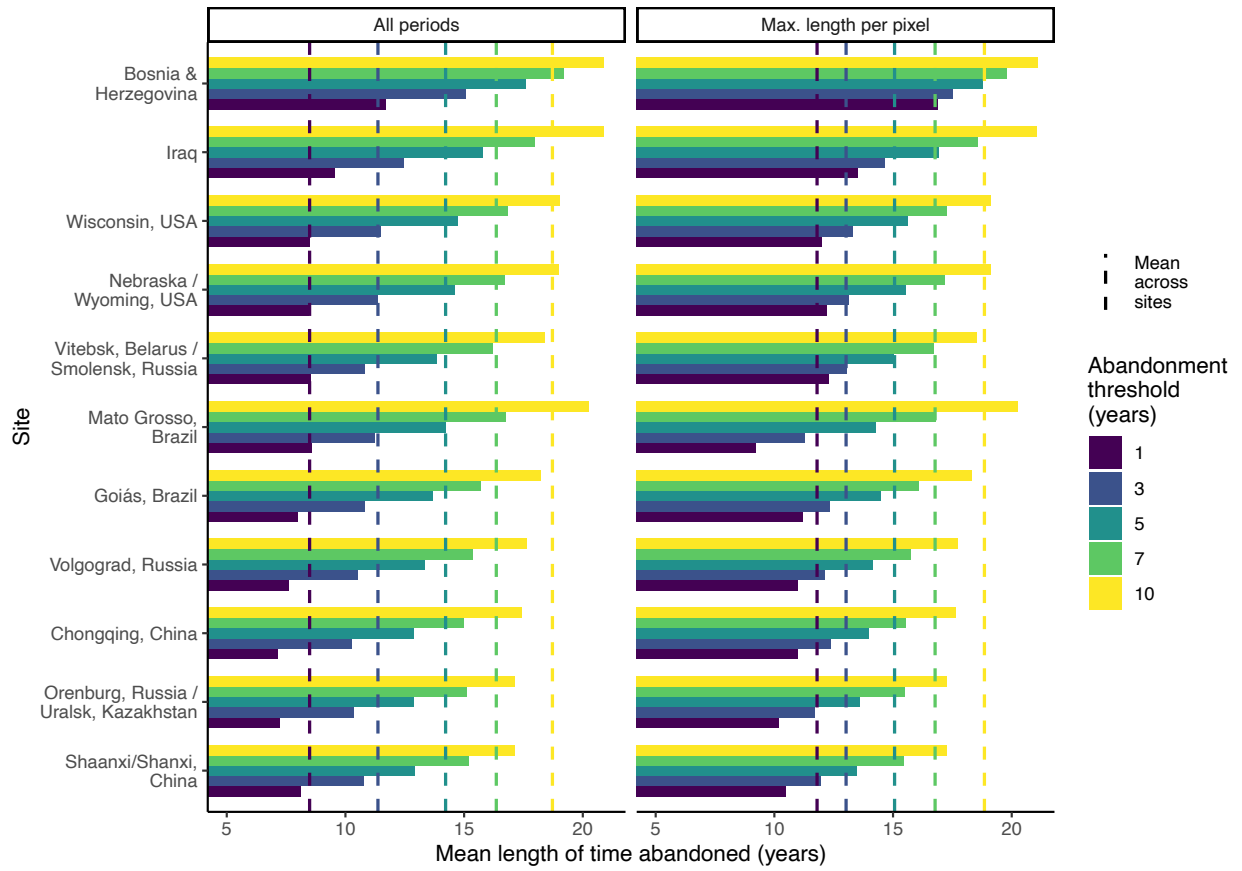
Fig. S21.

Mean abandonment lengths shown for various abandonment thresholds.
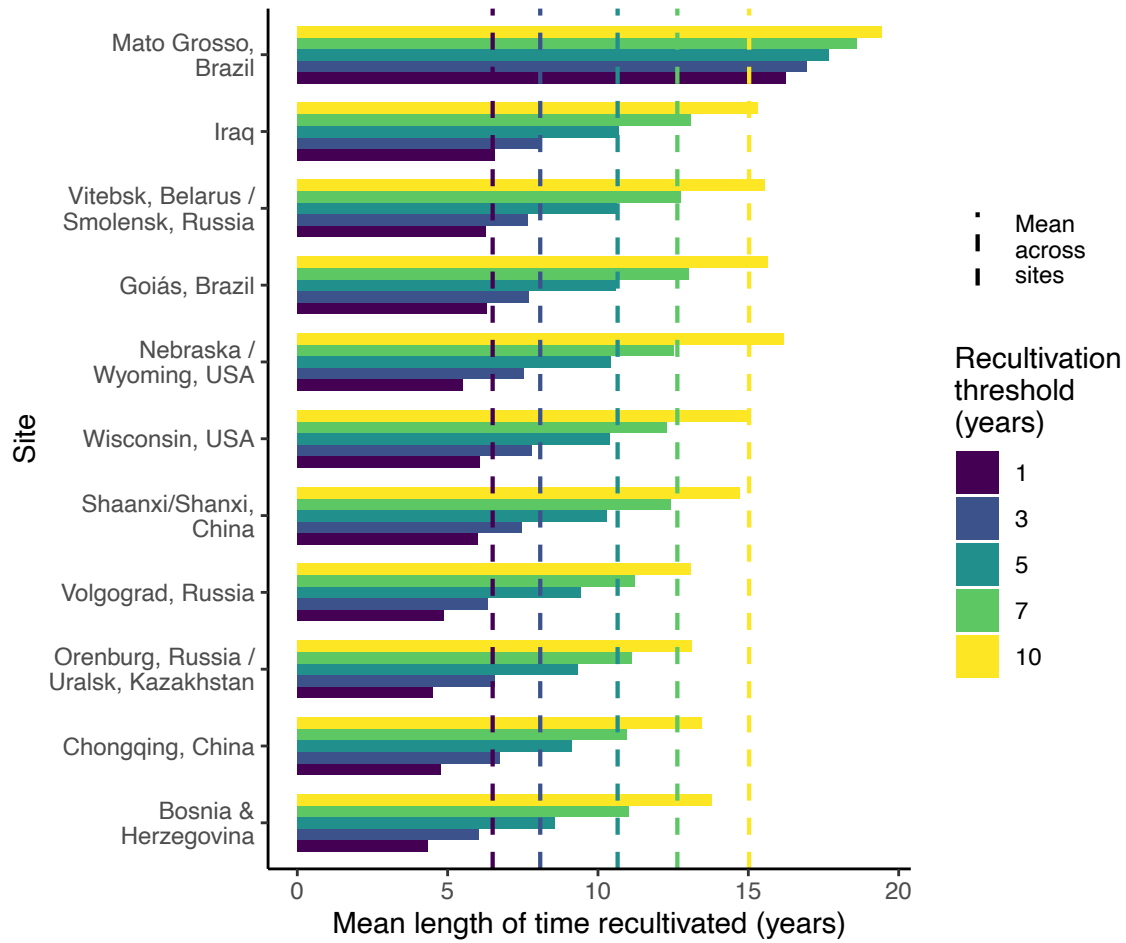
Fig. S22.

Mean recultivation duration at each site, shown for various recultivation thresholds.
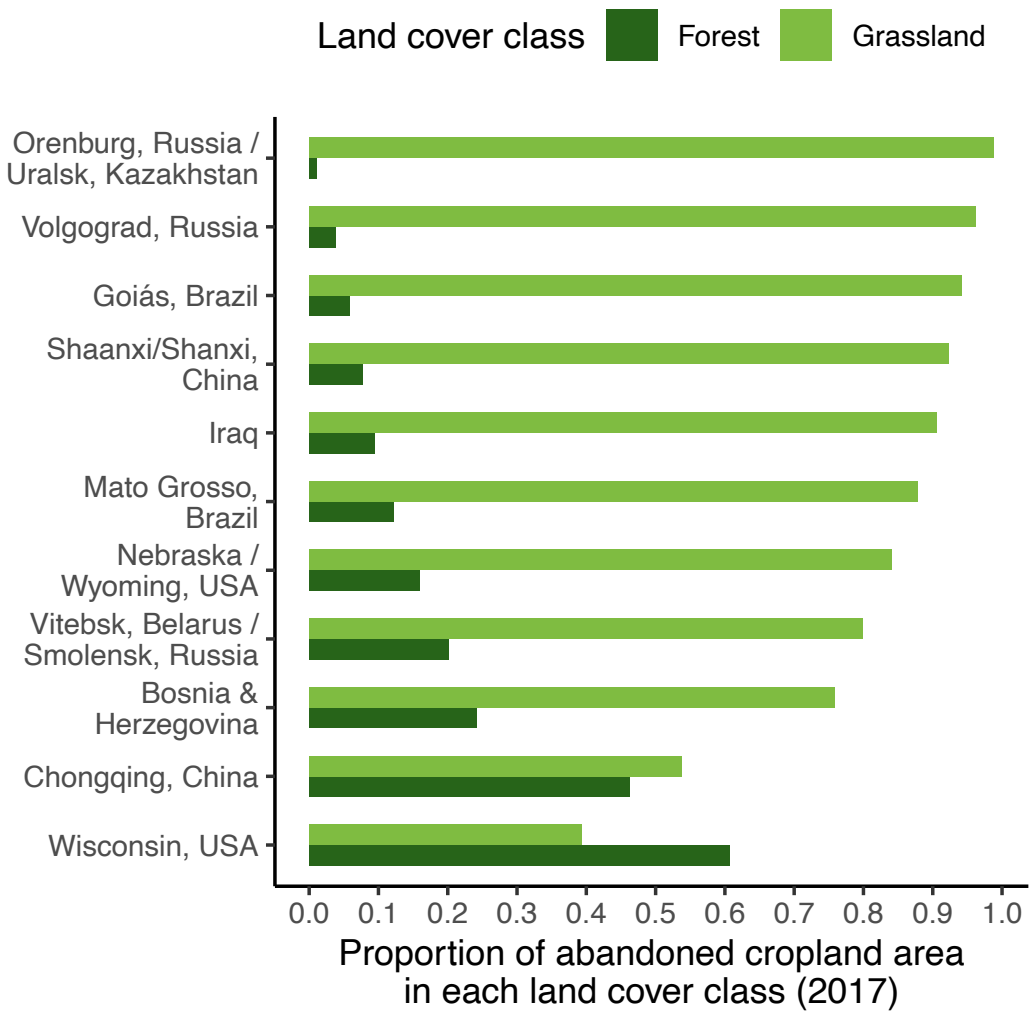
Fig. S23.

Proportion of abandoned cropland in each land cover class as of 2017.
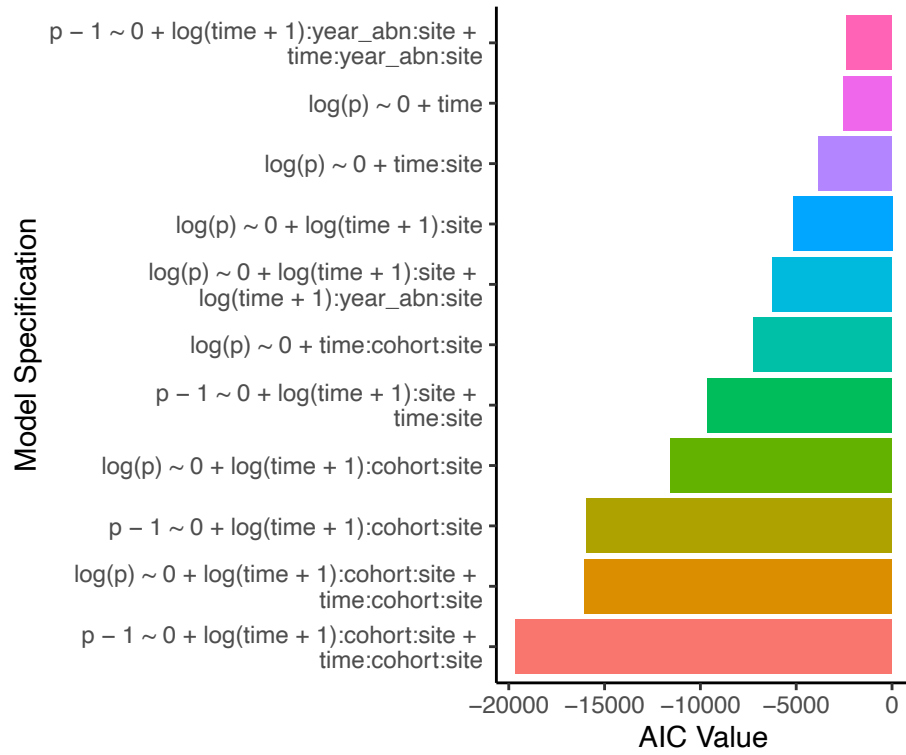
Fig. S24.

Akaike Information Criterion (AIC) values for various recultivation ("decay") model specifications polled across all 11 sites. Specifications included multiple combinations of site and cohort fixed effects, and linear and log transformations. More negative AIC values indicate a better model fit.
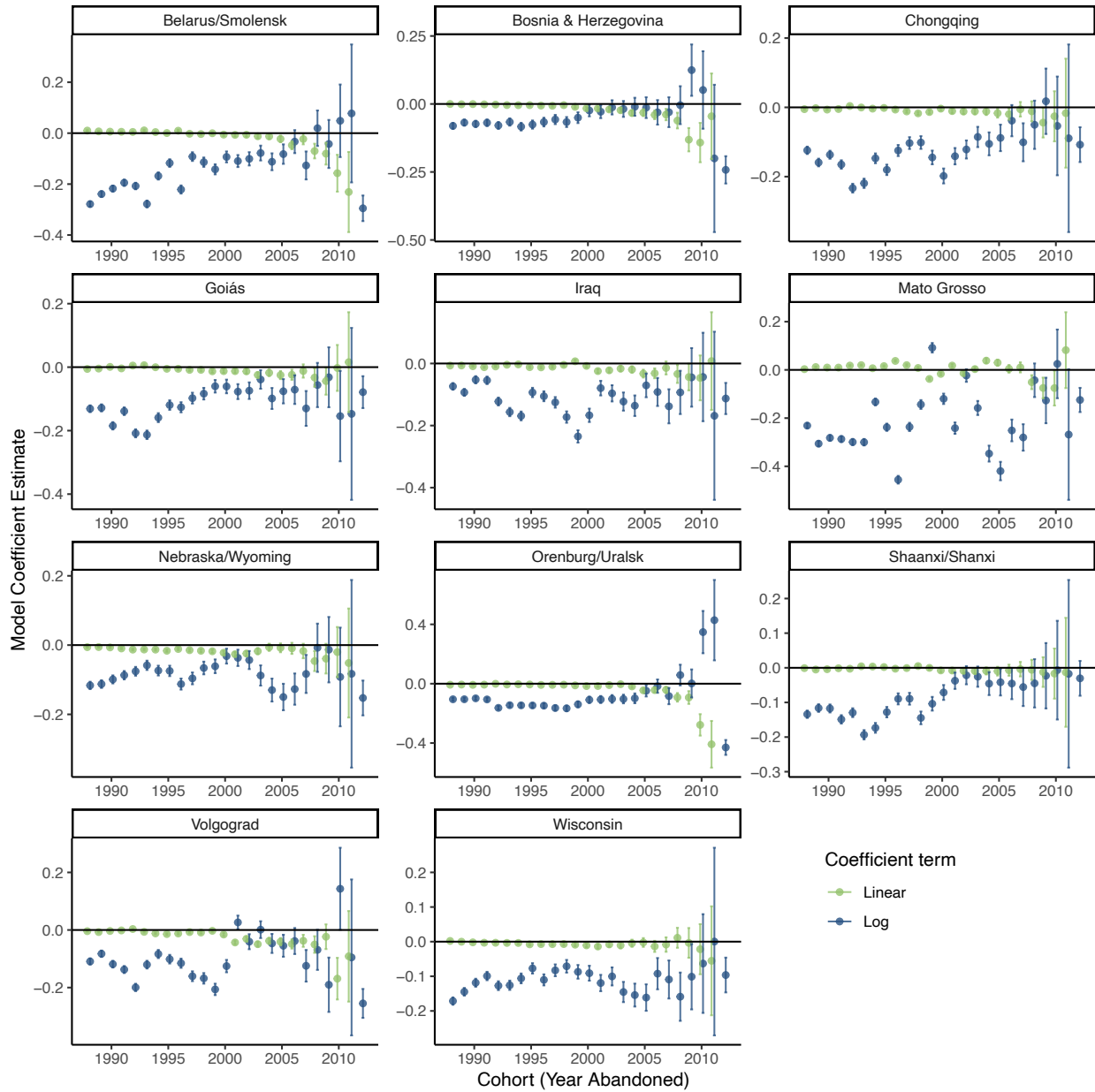
Fig. S25.

All model coefficients from our pooled model across all 11 sites, shown with associated uncertainty (95% confidence intervals).
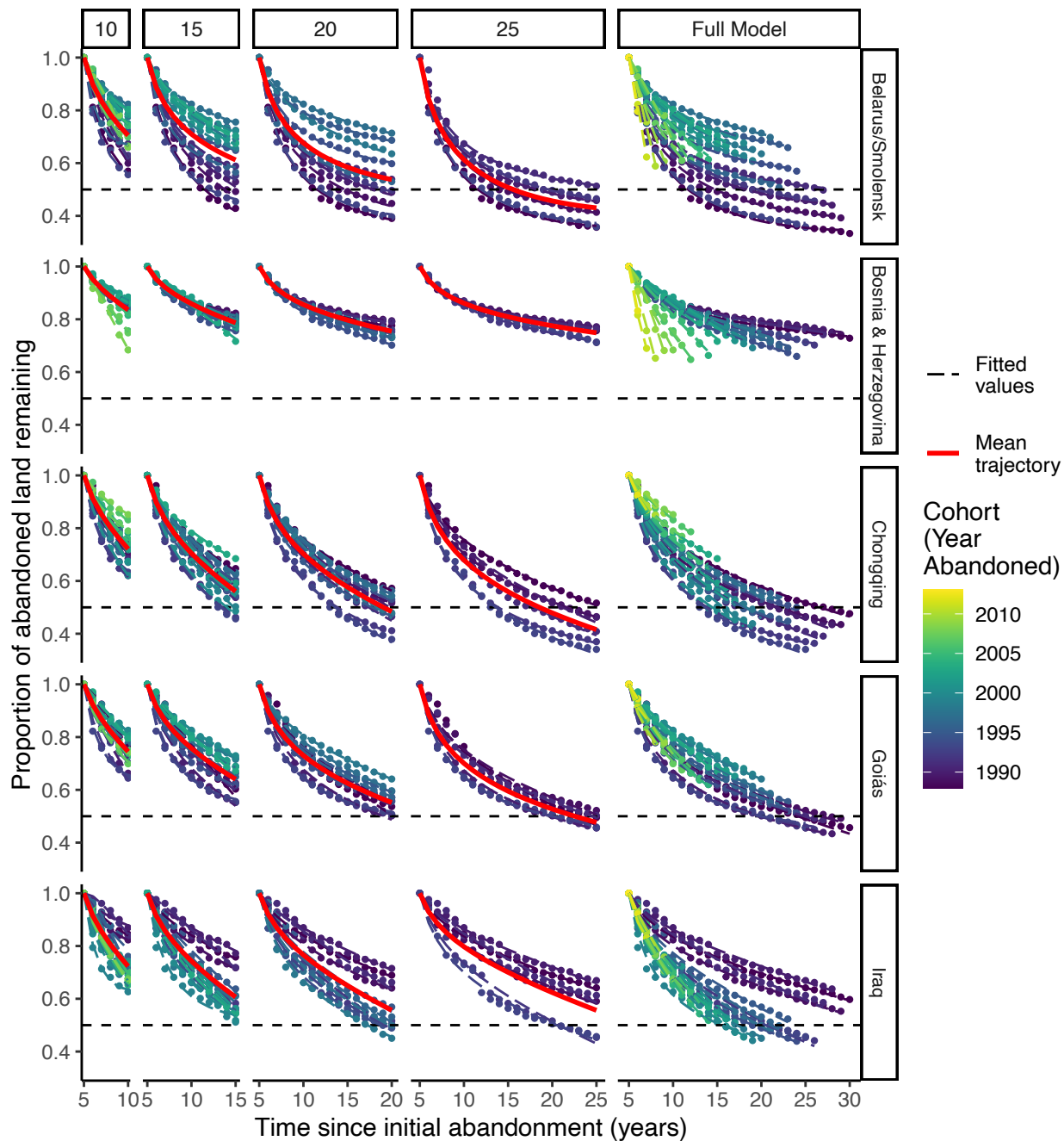
Fig. S26.

Recultivation ("decay") of abandoned croplands through time, modeled from subsets based on common endpoints, developed in order to make fair comparisons across cohorts. Observations are shown as points, and model decay trends are shown as dashed lines. Mean decay trajectories (shown in red) are calculated across selections of our data subset to four common endpoints (10, 15, 20, and 25 years in columns left to right) at each site, and the full dataset is shown in the rightmost column for comparison (corresponding to Fig. 6). These site mean decay trends were used to calculate the endpoint half-lives shown in Figs. 7 and S17. This figure shows our first five sites; the final six sites are shown in Fig. S27.
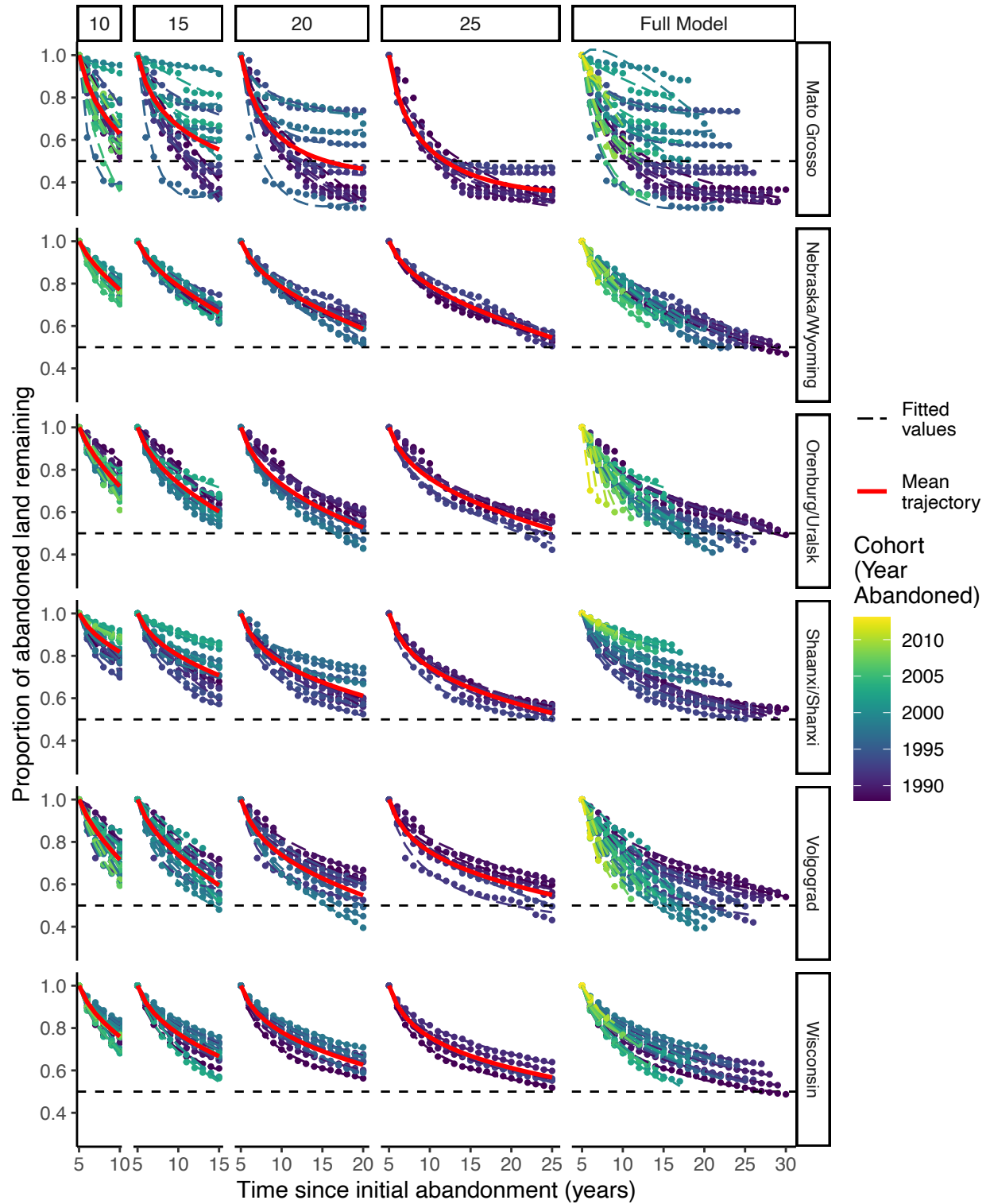
Fig. S27.

Companion figure to Fig. S26. Refer to associated caption to Fig. S26 above.
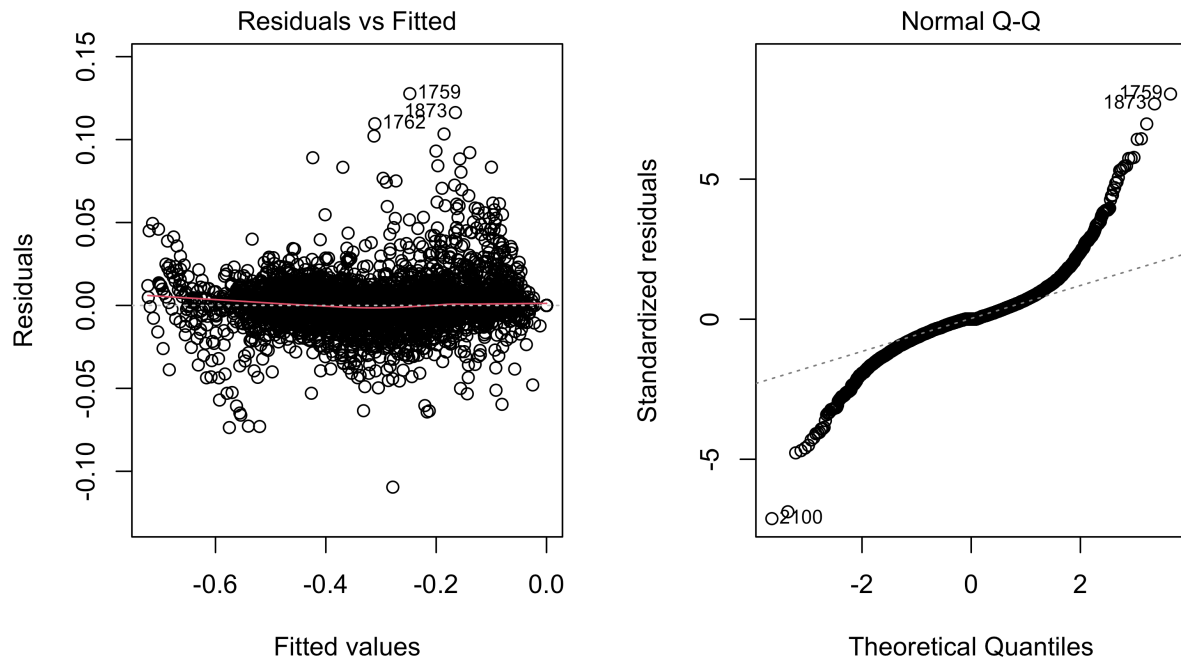
Fig. S28.

Diagnostic plots for our final linear model of the recultivation ("decay") of abandonment across sites. These models take the form shown in Equation (S2), and are shown in Fig. 6.
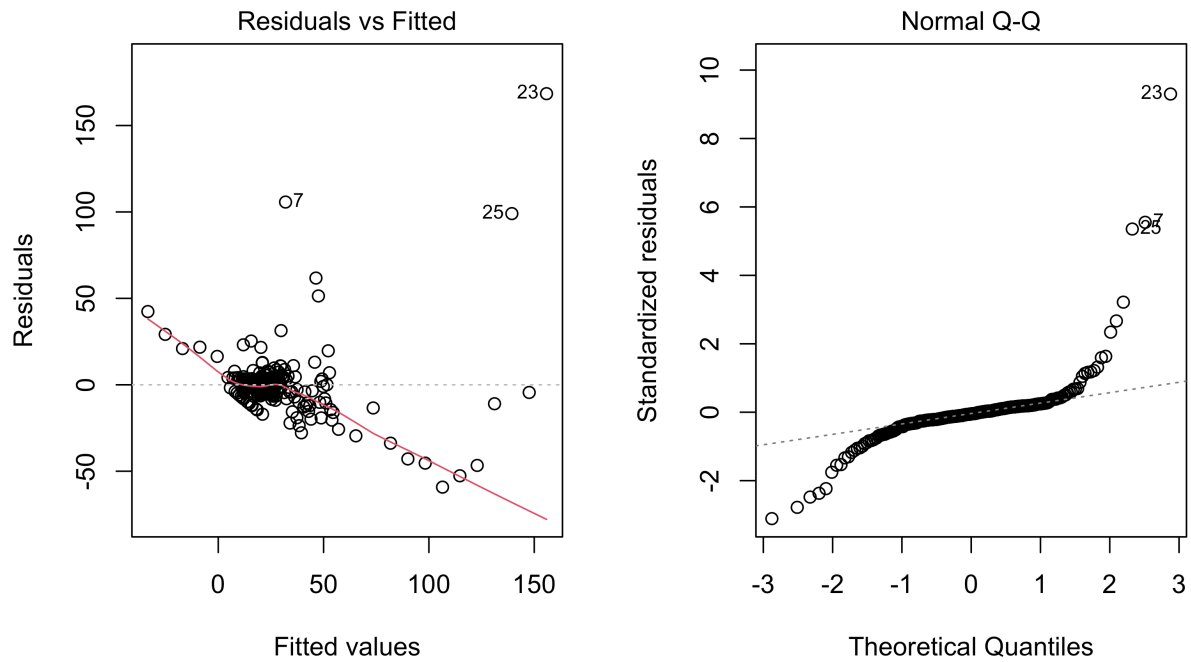
Fig. S29.

Residuals vs. fitted values (left) and QQ (right) diagnostic plots, for a simple `lm` call corresponding to Eq. (S3), in which the half-life (i.e., the time required for 50% of a given cohort of abandoned cropland to be recultivated) is modeled as a function of the year of initial abandonment at each site.

Section S4. Supplementary Tables

Table S1.

Observed area abandoned (Mha) as of 2017, potential area abandoned by 2017 (Mha) assuming no recultivation, the percent difference between observed and potential abandonment, and observed abandonment as of 2017 as a percent of the total cropland extent (i.e., the area of all lands that were cultivated at some point during the time series). This table replicates Figure S2. Note that sites are shown in descending order of area abandoned as of 2017 as a proportion of total cropland extent.

Site	Observed area (ha)	Potential area (ha)	Percent (%) difference from potential	Observed area as percent of total cropland extent
Bosnia & Herzegovina	729,061	913,573	-20.2%	47.45%
Vitebsk, Belarus / Smolensk, Russia	955,002	1,417,764	-32.64%	41.12%
Shaanxi/Shanxi, China	323,741	372,666	-13.13%	38.11%
Chongqing, China	440,088	591,493	-25.6%	36.78%
Iraq	388,234	579,324	-32.99%	35.45%
Goiás, Brazil	581,661	824,865	-29.48%	28.54%
Volgograd, Russia	855,385	1,399,165	-38.86%	25.4%
Orenburg, Russia / Uralsk, Kazakhstan	945,349	1,486,317	-36.4%	24.59%
Nebraska/Wyoming, USA	384,956	549,808	-29.98%	22.8%
Wisconsin, USA	445,963	603,201	-26.07%	20.8%
Mato Grosso, Brazil	11,277	25,273	-55.38%	0.59%
Total Across Sites	**6,060,717**	**8,763,449**	**-30.84%**	**27.55%**

Table S2.

Summary statistics describing the duration of abandonment (in years) at our eleven sites between 1987 and 2017, using a five-year abandonment definition, and incorporating all periods of abandonment (allowing for multiple per pixel).

Site	Mean	Median	Standard Deviation
Vitebsk, Belarus / Smolensk, Russia	13.85	12.00	7.56
Bosnia & Herzegovina	17.57	18.00	8.30
Chongqing, China	12.86	11.00	7.19
Goiás, Brazil	13.68	12.00	7.39
Iraq	15.79	13.00	8.80
Mato Grosso, Brazil	14.21	11.00	8.83
Nebraska/Wyoming, USA	14.61	13.00	7.81
Orenburg, Russia / Uralsk, Kazakhstan	12.86	11.00	6.93
Shaanxi/Shanxi, China	12.93	11.00	7.11
Volgograd, Russia	13.32	12.00	6.99
Wisconsin, USA	14.74	13.00	7.69
Mean across site summary statistics:	**14.22**	**12.45**	**7.69**
Standard deviation across site summary statistics:	**1.44**	**2.02**	**0.68**

Table S3.

Summary statistics describing the duration of potential abandonment (in years) for our scenario without recultivation, at our eleven sites between 1987 and 2017, using a five-year abandonment definition, and incorporating all periods of abandonment (allowing for multiple per pixel).

Site	Mean	Median	Standard Deviation
Vitebsk, Belarus / Smolensk, Russia	19.91	21.00	7.13
Bosnia & Herzegovina	21.32	23.00	7.01
Chongqing, China	18.15	19.00	7.75
Goiás, Brazil	18.50	18.00	7.50
Iraq	21.58	24.00	7.66
Mato Grosso, Brazil	23.42	27.00	7.41
Nebraska/Wyoming, USA	19.44	20.00	7.61
Orenburg, Russia / Uralsk, Kazakhstan	17.16	16.00	7.13
Shaanxi/Shanxi, China	15.70	14.00	7.94
Volgograd, Russia	18.13	18.00	6.52
Wisconsin, USA	19.20	20.00	7.13
Mean across site summary statistics:	**19.32**	**20.00**	**7.34**
Standard deviation across site summary statistics:	**2.18**	**3.69**	**0.41**

Table S4.

Summary statistics describing the duration of recultivation (in years) following qualifying periods of abandonment, at our eleven sites between 1987 and 2017, using a five-year abandonment definition and a one-year recultivation definition, and incorporating all periods of abandonment (allowing for multiple per pixel).

Site	Mean	Median	Standard Deviation
Vitebsk, Belarus / Smolensk, Russia	6.27	4.00	5.55
Bosnia & Herzegovina	4.34	3.00	3.89
Chongqing, China	4.76	3.00	4.27
Goiás, Brazil	6.30	4.00	5.51
Iraq	6.56	4.00	5.61
Mato Grosso, Brazil	16.25	18.00	6.83
Nebraska/Wyoming, USA	5.51	3.00	5.32
Orenburg, Russia / Uralsk, Kazakhstan	4.50	3.00	4.19
Shaanxi/Shanxi, China	6.02	4.00	5.18
Volgograd, Russia	4.88	3.00	4.13
Wisconsin, USA	6.08	4.00	5.37
Mean across site summary statistics:	**6.50**	**4.82**	**5.08**
Standard deviation across site summary statistics:	**3.33**	**4.40**	**0.88**

Table S5.

Estimated carbon sequestration in observed and potential area abandoned by 2017, reported in terms of Mg C, as the percent difference between observed and potential accumulation, and as Mg C per ha.

Site	Carbon (Mg C, observed)	Carbon (Mg C, potential)	Carbon (% diff. from potential)	Mg C per ha, observed	Mg C per ha, potential
Orenburg, Russia / Uralsk, Kazakhstan	1,408,615	2,441,480	-42.3%	1.49	1.64
Volgograd, Russia	1,992,475	3,600,480	-44.66%	2.33	2.57
Nebraska/Wyoming, USA	978,183	1,585,435	-38.3%	2.54	2.88
Iraq	1,033,200	1,706,143	-39.44%	2.66	2.95
Shaanxi/Shanxi, China	1,111,329	1,597,280	-30.42%	3.43	4.29
Goiás, Brazil	5,540,867	9,219,905	-39.9%	9.53	11.18
Wisconsin, USA	12,649,527	18,790,418	-32.68%	28.36	31.15
Vitebsk, Belarus / Smolensk, Russia	32,409,304	54,893,670	-40.96%	33.94	38.72
Bosnia & Herzegovina	31,352,027	40,839,454	-23.23%	43.00	44.70
Chongqing, China	20,810,701	34,182,793	-39.12%	47.29	57.79
Mato Grosso, Brazil	548,729	1,127,313	-51.32%	48.66	44.61
Total Across Sites	**109,834,956**	**169,984,370**	**-35.39%**	**18.12**	**19.40**

Table S6.

Cropland abandonment (in Mha) as of 2017 as identified using a) our annual time series and a five-year abandonment definition and b) a two-year method taking the difference between land cover in 1987 and 2017.

Site	Area (annual, as of 2017)	Area (two year: 2017-1987)	Percent % from annual area	Jaccard Similarity	Percent Area <5 Years Old (two year)
Goiás, Brazil	581,661	319,499	-45.07%	0.29	24.01%
Chongqing, China	440,088	273,839	-37.78%	0.38	26.78%
Vitebsk, Belarus / Smolensk, Russia	955,002	655,689	-31.34%	0.50	16.83%
Nebraska/Wyoming, USA	384,956	274,133	-28.79%	0.48	16.69%
Bosnia & Herzegovina	729,061	569,091	-21.94%	0.63	10.36%
Wisconsin, USA	445,963	358,420	-19.63%	0.45	28.57%
Iraq	388,234	348,152	-10.32%	0.55	22.92%
Volgograd, Russia	855,385	857,989	0.3%	0.46	33.35%
Orenburg, Russia / Uralsk, Kazakhstan	945,349	975,131	3.15%	0.52	28.92%
Shaanxi/Shanxi, China	323,741	355,581	9.83%	0.51	28.3%
Mato Grosso, Brazil	11,277	16,507	46.38%	0.29	0.69%

REFERENCES AND NOTES

1. E. W. Sanderson, J. Walston, J. G. Robinson, From bottleneck to breakthrough: Urbanization and the future of biodiversity conservation. *BioScience* **68**, 412–426 (2018).

2. J. Rey Benayas, A. Martins, J. M. Nicolau, J. Schulz, Abandonment of agricultural land: An overview of drivers and consequences. *CAB Rev. Perspect. Agric. Vet. Sci. Nutr. Nat. Resour.* **2**, 14 (2007).

3. A. V. Prishchepov, F. Schierhorn, F. Löw, Unraveling the diversity of trajectories and drivers of global agricultural land abandonment. *Land* **10**, 97 (2021).

4. J. S. Næss, O. Cavalett, F. Cherubini, The land–energy–water nexus of global bioenergy potentials from abandoned cropland. *Nat. Sustain.* **4**, 525–536 (2021).

5. S. Li, X. Li, Global understanding of farmland abandonment: A review and prospects. *J. Geogr. Sci.* **27**, 1123–1150 (2017).

6. R. L. Chazdon, D. Lindenmayer, M. R. Guariguata, R. Crouzeilles, J. M. Rey Benayas, E. Lazos Chavero, Fostering natural forest regeneration on former agricultural land through economic and policy interventions. *Environ. Res. Lett.* **15**, 043002 (2020).

7. P. Potapov, S. Turubanova, M. C. Hansen, A. Tyukavina, V. Zalles, A. Khan, X. P. Song, A. Pickens, Q. Shen, J. Cortez, Global maps of cropland extent and change show accelerated cropland expansion in the twenty-first century. *Nature Food* **3**, 19–28 (2022).

8. S. Roe, C. Streck, M. Obersteiner, S. Frank, B. Griscom, L. Drouet, O. Fricko, M. Gusti, N. Harris, T. Hasegawa, Z. Hausfather, P. Havlík, J. House, G.-J. Nabuurs, A. Popp, M. J. S. Sánchez, J. Sanderman, P. Smith, E. Stehfest, D. Lawrence, Contribution of the land sector to a 1.5 °C world. *Nat. Clim. Chang.* **9**, 817–828 (2019).

9. D. Tilman, M. Clark, D. R. Williams, K. Kimmel, S. Polasky, C. Packer, Future threats to biodiversity and pathways to their prevention. *Nature* **546**, 73–81 (2017).

10. Z. Xie, E. T. Game, R. J. Hobbs, D. J. Pannell, S. R. Phinn, E. McDonald-Madden, Conservation opportunities on uncontested lands. *Nat. Sustain.* **3**, 9–15 (2019).

11. L. M. Navarro, H. M. Pereira, Rewilding abandoned landscapes in Europe. *Ecosystems* **15**, 900–912 (2012).

12. R. L. Chazdon, E. N. Broadbent, D. M. A. Rozendaal, F. Bongers, A. M. A. Zambrano, T. M. Aide, P. Balvanera, J. M. Becknell, V. Boukili, P. H. S. Brancalion, D. Craven, J. S. Almeida-Cortez, G. A. L. Cabral, B. de Jong, J. S. Denslow, D. H. Dent, S. J. DeWalt, J. M. Dupuy, S. M. Durán, M. M. Espírito-Santo, M. C. Fandino, R. G. César, J. S. Hall, J. L. Hernández-Stefanoni, C. C. Jakovac, A. B. Junqueira, D. Kennard, S. G. Letcher, M. Lohbeck, M. Martínez-Ramos, P. Massoca, J. A. Meave, R. Mesquita, F. Mora, R. Muñoz, R. Muscarella, Y. R. F. Nunes, S. Ochoa-Gaona, E. Orihuela-Belmonte, M. Peña-Claros, E. A. Pérez-García, D. Piotto, J. S. Powers, J. Rodríguez-Velazquez, I. E. Romero-Pérez, J. Ruíz, J. G. Saldarriaga, A. Sanchez-Azofeifa, N. B. Schwartz, M. K. Steininger, N. G. Swenson, M. Uriarte, M. van Breugel, H. van der Wal, M. D. M. Veloso, H. Vester, I. C. G. Vieira, T. V. Bentos, G. B. Williamson, L. Poorter, Carbon sequestration potential of second-growth forest regeneration in the Latin American tropics. *Sci. Adv.* **2**, e1501639 (2016).

13. Y. Yang, D. Tilman, G. Furey, C. Lehman, Soil carbon sequestration accelerated by restoration of grassland biodiversity. *Nat. Commun.* **10**, 1–7 (2019).

14. IPCC, V. Masson-Delmotte, P. Zhai, H.-O. Pörtner, D. Roberts, J. Skea, P. R. Shukla, A. Pirani, W. Moufouma-Okia, C. Péan, R. Pidcock, S. Connors, J. B. R. Matthews, Y. Chen, X. Zhou, M. I. Gomis, E. Lonnoy, T. Maycock, M. Tignor, T. Waterfield, Eds., Global Warming of 1.5°C. An IPCC Special Report on the impacts of global warming of 1.5°C above pre-industrial levels and related global greenhouse gas emission pathways, in the context of strengthening the global response to the threat of climate change, sustainable development, and efforts to eradicate poverty (IPCC, 2018).

15. A. Popp, K. Calvin, S. Fujimori, P. Havlik, F. Humpenöder, E. Stehfest, B. L. Bodirsky, J. P. Dietrich, J. C. Doelmann, M. Gusti, T. Hasegawa, P. Kyle, M. Obersteiner, A. Tabeau, K. Takahashi, H. Valin, S. Waldhoff, I. Weindl, M. Wise, E. Kriegler, H. Lotze-Campen, O. Fricko, K. Riahi, D. P. van Vuuren, Land-use futures in the shared socio-economic pathways. *Glob. Environ. Change* **42**, 331–345 (2017).

16. R. A. Houghton, A. A. Nassikas, Negative emissions from stopping deforestation and forest degradation, globally. *Glob. Chang. Biol.* **24**, 350–359 (2018).

17. J. E. Campbell, D. B. Lobell, R. C. Genova, C. B. Field, The global potential of bioenergy on abandoned agriculture lands. *Environ. Sci. Technol.* **42**, 5791–5794 (2008).

18. G. P. Robertson, S. K. Hamilton, B. L. Barham, B. E. Dale, R. C. Izaurralde, R. D. Jackson, D. A. Landis, S. M. Swinton, K. D. Thelen, J. M. Tiedje, Cellulosic biofuel contributions to a sustainable energy future: Choices and outcomes. *Science* **356**, eaal2324 (2017).

19. R. C. Henry, P. Alexander, S. Rabin, P. Anthoni, M. D. A. Rounsevell, A. Arneth, The role of global dietary transitions for safeguarding biodiversity. *Glob. Environ. Change* **58**, 101956 (2019).

20. D. Leclère, M. Obersteiner, M. Barrett, S. H. M. Butchart, A. Chaudhary, A. De Palma, F. A. J. DeClerck, M. Di Marco, J. C. Doelman, M. Dürauer, R. Freeman, M. Harfoot, T. Hasegawa, S. Hellweg, J. P. Hilbers, S. L. L. Hill, F. Humpenöder, N. Jennings, T. Krisztin, G. M. Mace, H. Ohashi, A. Popp, A. Purvis, A. M. Schipper, A. Tabeau, H. Valin, H. van Meijl, W.-J. van Zeist, P. Visconti, R. Alkemade, R. Almond, G. Bunting, N. D. Burgess, S. E. Cornell, F. Di Fulvio, S. Ferrier, S. Fritz, S. Fujimori, M. Grooten, T. Harwood, P. Havlík, M. Herrero, A. J. Hoskins, M. Jung, T. Kram, H. Lotze-Campen, T. Matsui, C. Meyer, D. Nel, T. Newbold, G. Schmidt-Traub, E. Stehfest, B. B. N. Strassburg, D. P. van Vuuren, C. Ware, J. E. M. Watson, W. Wu, L. Young, Bending the curve of terrestrial biodiversity needs an integrated strategy. *Nature* **585**, 551–556 (2020).

21. C. Folberth, N. Khabarov, J. Balkovič, R. Skalský, P. Visconti, P. Ciais, I. A. Janssens, J. Peñuelas, M. Obersteiner, The global cropland-sparing potential of high-yield farming. *Nat. Sustain.* **3**, 281–289 (2020).

22. P. Meyfroidt, E. F. Lambin, Global forest transition: Prospects for an end to deforestation. *Annu. Rev. Env. Resour.* **36**, 343–371 (2011).

23. T. K. Rudel, P. Meyfroidt, R. Chazdon, F. Bongers, S. Sloan, H. R. Grau, T. Van Holt, L. Schneider, Whither the forest transition? Climate change, policy responses, and redistributed forests in the twenty-first century. *Ambio* **49**, 74–84 (2020).

24. N. B. Schwartz, T. M. Aide, J. Graesser, H. R. Grau, M. Uriarte, Reversals of reforestation across Latin America limit climate mitigation potential of tropical forests. *Front. For. Glob. Change* **3**, 1–10 (2020).

25. S. Sloan, Reforestation reversals and forest transitions. *Land Use Policy* **112**, 105800 (2022).

26. D. M. A. Rozendaal, F. Bongers, T. M. Aide, E. Alvarez-Dávila, N. Ascarrunz, P. Balvanera, J. M. Becknell, T. V. Bentos, P. H. S. Brancalion, G. A. L. Cabral, S. Calvo-Rodriguez, J. Chave, R. G. César, R. L.

Chazdon, R. Condit, J. S. Dallinga, J. S. de Almeida-Cortez, B. de Jong, A. de Oliveira, J. S. Denslow, D. H. Dent, S. J. DeWalt, J. M. Dupuy, S. M. Durán, L. P. Dutrieux, M. M. Espírito-Santo, M. C. Fandino, G. W. Fernandes, B. Finegan, H. García, N. Gonzalez, V. G. Moser, J. S. Hall, J. L. Hernández-Stefanoni, S. Hubbell, C. C. Jakovac, A. J. Hernández, A. B. Junqueira, D. Kennard, D. Larpin, S. G. Letcher, J. Licona, E. Lebrija-Trejos, E. Marín-Spiotta, M. Martínez-Ramos, P. E. S. Massoca, J. A. Meave, R. C. G. Mesquita, F. Mora, S. C. Müller, R. Muñoz, S. N. de Oliveira Neto, N. Norden, Y. R. F. Nunes, S. Ochoa-Gaona, E. Ortiz-Malavassi, R. Ostertag, M. Peña-Claros, E. A. Pérez-García, D. Piotto, J. S. Powers, J. Aguilar-Cano, S. Rodriguez-Buritica, J. Rodríguez-Velázquez, M. A. Romero-Romero, J. Ruíz, A. Sanchez-Azofeifa, A. S. de Almeida, W. L. Silver, N. B. Schwartz, W. W. Thomas, M. Toledo, M. Uriarte, E. V. de Sá Sampaio, M. van Breugel, H. van der Wal, S. V. Martins, M. D. M. Veloso, H. F. M. Vester, A. Vicentini, I. C. G. Vieira, P. Villa, G. B. Williamson, K. J. Zanini, J. Zimmerman, L. Poorter, Biodiversity recovery of Neotropical secondary forests. *Sci. Adv.* **5**, eaau3114 (2019).

27. O. Acevedo-Charry, T. M. Aide, Recovery of amphibian, reptile, bird and mammal diversity during secondary forest succession in the tropics. *Oikos* **128**, 1065–1078 (2019).

28. F. Isbell, D. Tilman, P. B. Reich, A. T. Clark, Deficits of biodiversity and productivity linger a century after agricultural abandonment. *Nat. Ecol. Evol.* **3**, 1533–1538 (2019).

29. A. N. Nerlekar, J. W. Veldman, High plant diversity and slow assembly of old-growth grasslands. *Proc. Natl. Acad. Sci. U.S.A.* **117**, 18550–18556 (2020).

30. J. J. Gilroy, P. Woodcock, F. A. Edwards, C. Wheeler, B. L. G. Baptiste, C. A. Medina Uribe, T. Haugaasen, D. P. Edwards, Cheap carbon and biodiversity co-benefits from forest regeneration in a hotspot of endemism. *Nat. Clim. Chang.* **4**, 503–507 (2014).

31. S. C. Cook-Patton, S. M. Leavitt, D. Gibbs, N. L. Harris, K. Lister, K. J. Anderson-Teixeira, R. D. Briggs, R. L. Chazdon, T. W. Crowther, P. W. Ellis, H. P. Griscom, V. Herrmann, K. D. Holl, R. A. Houghton, C. Larrosa, G. Lomax, R. Lucas, P. Madsen, Y. Malhi, A. Paquette, J. D. Parker, K. Paul, D. Routh, S. Roxburgh, S. Saatchi, J. van den Hoogen, W. S. Walker, C. E. Wheeler, S. A. Wood, L. Xu, B. W. Griscom, Mapping carbon accumulation potential from global natural forest regrowth. *Nature* **585**, 545–550 (2020).

32. L. Poorter, F. Bongers, T. M. Aide, A. M. A. Zambrano, P. Balvanera, J. M. Becknell, V. Boukili, P. H. S. Brancalion, E. N. Broadbent, R. L. Chazdon, D. Craven, J. S. De Almeida-Cortez, G. A. L. Cabral, B. H. J. De Jong, J. S. Denslow, D. H. Dent, S. J. DeWalt, J. M. Dupuy, S. M. Durán, M. M. Espírito-Santo, M. C. Fandino, R. G. César, J. S. Hall, J. L. Hernandez-Stefanoni, C. C. Jakovac, A. B. Junqueira, D. Kennard, S. G. Letcher, J. C. Licona, M. Lohbeck, E. Marín-Spiotta, M. Martínez-Ramos, P. Massoca, J. A. Meave, R. Mesquita, F. Mora, R. Munõz, R. Muscarella, Y. R. F. Nunes, S. Ochoa-Gaona, A. A. De Oliveira, E. Orihuela-Belmonte, M. Penã-Claros, E. A. Pérez-Garciá, D. Piotto, J. S. Powers, J. Rodríguez-Velázquez, I. E. Romero-Pérez, J. Ruíz, J. G. Saldarriaga, A. Sanchez-Azofeifa, N. B. Schwartz, M. K. Steininger, N. G. Swenson, M. Toledo, M. Uriarte, M. Van Breugel, H. Van Der Wal, M. D. M. Veloso, H. F. M. Vester, A. Vicentini, I. C. G. Vieira, T. V. Bentos, G. B. Williamson, D. M. A. Rozendaal, Biomass resilience of Neotropical secondary forests. *Nature* **530**, 211–214 (2016).

33. D. K. Munroe, D. B. van Berkel, P. H. Verburg, J. L. Olson, Alternative trajectories of land abandonment: Causes, consequences and research challenges. *Curr. Opin. Environ. Sustain.* **5**, 471–476 (2013).

34. C. Alcantara, T. Kuemmerle, M. Baumann, E. V. Bragina, P. Griffiths, P. Hostert, J. Knorn, D. Müller, A. V. Prishchepov, F. Schierhorn, A. Sieber, V. C. Radeloff, Mapping the extent of abandoned farmland in Central and Eastern Europe using MODIS time series satellite data. *Environ. Res. Lett.* **8**, 035035 (2013).

35. S. Estel, T. Kuemmerle, C. Alcántara, C. Levers, A. Prishchepov, P. Hostert, Mapping farmland abandonment and recultivation across Europe using MODIS NDVI time series. *Remote Sens. Environ.* **163**, 312–325 (2015).

36. T. J. Lark, J. M. Salmon, H. K. Gibbs, Cropland expansion outpaces agricultural and biofuel policies in the United States. *Environ. Res. Lett.* **10**, 044003 (2015).

37. A. Dara, M. Baumann, T. Kuemmerle, D. Pflugmacher, A. Rabe, P. Griffiths, N. Hölzel, J. Kamp, M. Freitag, P. Hostert, Mapping the timing of cropland abandonment and recultivation in northern Kazakhstan using annual Landsat time series. *Remote Sens. Environ.* **213**, 49–60 (2018).

38. H. Yin, A. Brandão, J. Buchner, D. Helmers, B. G. Iuliano, N. E. Kimambo, K. E. Lewińska, E. Razenkova, A. Rizayeva, N. Rogova, S. A. Spawn, Y. Xie, V. C. Radeloff, Monitoring cropland abandonment with Landsat time series. *Remote Sens. Environ.* **246**, 111873 (2020).

39. J. Sanderman, D. Woolf, J. Lehmann, C. Rivard, L. Poggio, G. Heuvelink, D. Bossio, Soils Revealed soil carbon futures (2020). doi:10.7910/DVN/HA17D3.

40. J. L. Reid, M. E. Fagan, J. Lucas, J. Slaughter, R. A. Zahawi, The ephemerality of secondary forests in southern Costa Rica. *Conserv. Lett.* **12**, e12607 (2019).

41. S. Nunes, L. Oliveira, J. Siqueira, D. C. Morton, C. M. Souza, Unmasking secondary vegetation dynamics in the Brazilian Amazon. *Environ. Res. Lett.* **15**, 034057 (2020).

42. C. C. Smith, F. D. B. Espírito-Santo, J. R. Healey, P. J. Young, G. D. Lennox, J. Ferreira, J. Barlow, Secondary forests offset less than 10% of deforestation-mediated carbon emissions in the Brazilian Amazon. *Global Chang. Biol.* **6**, gcb.15352 (2020).

43. C. Vancutsem, F. Achard, J.-F. Pekel, G. Vieilledent, S. Carboni, D. Simonetti, J. Gallego, L. E. O. C. Aragão, R. Nasi, Long-term (1990–2019) monitoring of forest cover changes in the humid tropics. *Sci. Adv.* **7**, 1–22 (2021).

44. P. Meyfroidt, F. Schierhorn, A. V. Prishchepov, D. Müller, T. Kuemmerle, Drivers, constraints and trade-offs associated with recultivating abandoned cropland in Russia, Ukraine and Kazakhstan. *Glob. Environ. Change* **37**, 1–15 (2016).

45. P. Meli, K. D. Holl, J. M. Rey Benayas, H. P. Jones, P. C. Jones, D. Montoya, D. Moreno Mateos, A global review of past land use, climate, and active vs. passive restoration effects on forest recovery. *PLOS ONE* **12**, e0171368 (2017).

46. J. L. Reid, M. E. Fagan, R. A. Zahawi, Positive site selection bias in meta-analyses comparing natural regeneration to active forest restoration. *Sci. Adv.* **4**, 1–4 (2018).

47. V. Arroyo-Rodríguez, F. P. L. Melo, M. Martínez-Ramos, F. Bongers, R. L. Chazdon, J. A. Meave, N. Norden, B. A. Santos, I. R. Leal, M. Tabarelli, Multiple successional pathways in human-modified tropical landscapes: New insights from forest succession, forest fragmentation and landscape ecology research. *Biol. Rev.* **92**, 326–340 (2017).

48. R. Crouzeilles, M. Curran, M. S. Ferreira, D. B. Lindenmayer, C. E. V. Grelle, J. M. Rey Benayas, A global meta-analysis on the ecological drivers of forest restoration success. *Nat. Commun.* **7**, 11666 (2016).

49. N. Norden, H. A. Angarita, F. Bongers, M. Martínez-Ramos, I. Granzow-de la Cerda, M. van Breugel, E. Lebrija-Trejos, J. A. Meave, J. Vandermeer, G. B. Williamson, B. Finegan, R. Mesquita, R. L. Chazdon,

Successional dynamics in Neotropical forests are as uncertain as they are predictable. *Proc. Natl. Acad. Sci. U.S.A.* **112**, 8013–8018 (2015).

50. H. P. Jones, O. J. Schmitz, Rapid recovery of damaged ecosystems. *PLOS ONE* **4**, e5653 (2009).

51. I. Kämpf, W. Mathar, I. Kuzmin, N. Hölzel, K. Kiehl, Post-Soviet recovery of grassland vegetation on abandoned fields in the forest steppe zone of Western Siberia. *Biodivers. Conserv.* **25**, 2563–2580 (2016).

52. J. Kamp, R. Urazaliev, P. F. Donald, N. Hölzel, Post-Soviet agricultural change predicts future declines after recent recovery in Eurasian steppe bird populations. *Biol. Conserv.* **144**, 2607–2614 (2011).

53. P. A. Martin, A. C. Newton, J. M. Bullock, Carbon pools recover more quickly than plant biodiversity in tropical secondary forests. *Proc. R. Soc. B Biol. Sci.* **280**, 20132236 (2013).

54. P. R. Piffer, A. Calaboni, M. R. Rosa, N. B. Schwartz, L. R. Tambosi, M. Uriarte, Ephemeral forest regeneration limits carbon sequestration potential in the Brazilian Atlantic Forest. *Global Chang. Biol.*, 630–643 (2021).

55. R. Lal, Soil carbon sequestration impacts on global climate change and food security. *Science* **304**, 1623–1627 (2004).

56. T.-M. Wertebach, N. Hölzel, I. Kämpf, A. Yurtaev, S. Tupitsin, K. Kiehl, J. Kamp, T. Kleinebecker, Soil carbon sequestration due to post-Soviet cropland abandonment: Estimates from a large-scale soil organic carbon field inventory. *Global Chang. Biol.* **23**, 3729–3741 (2017).

57. V. A. Cramer, R. J. Hobbs, R. J. Standish, What's new about old fields? Land abandonment and ecosystem assembly. *Trends Ecol. Evol.* **23**, 104–112 (2008).

58. T. Parkhurst, S. M. Prober, R. J. Hobbs, R. J. Standish, Global meta-analysis reveals incomplete recovery of soil conditions and invertebrate assemblages after ecological restoration in agricultural landscapes. *J. Appl. Ecol.* **59**, 358–372 (2021).

59. R. L. Chazdon, M. R. Guariguata, Natural regeneration as a tool for large-scale forest restoration in the tropics: Prospects and challenges. *Biotropica* **48**, 716–730 (2016).

60. C. Queiroz, R. Beilin, C. Folke, R. Lindborg, Farmland abandonment: Threat or opportunity for biodiversity conservation? A global review. *Front. Ecol. Environ.* **12**, 288–296 (2014).

61. C. Sirami, L. Brotons, I. Burfield, J. Fonderflick, J. L. Martin, Is land abandonment having an impact on biodiversity? A meta-analytical approach to bird distribution changes in the north-western Mediterranean. *Biol. Conserv.* **141**, 450–459 (2008).

62. P. Batáry, L. V. Dicks, D. Kleijn, W. J. Sutherland, The role of agri-environment schemes in conservation and environmental management. *Conserv. Biol.* **29**, 1006–1016 (2015).

63. C. M. J. Fayet, K. H. Reilly, C. Van Ham, P. H. Verburg, What is the future of abandoned agricultural lands? A systematic review of alternative trajectories in Europe. *Land Use Policy* **112**, 105833 (2022).

64. C. Levers, D. Müller, K. Erb, H. Haberl, M. R. Jepsen, M. J. Metzger, P. Meyfroidt, T. Plieninger, C. Plutzar, J. Stürck, P. H. Verburg, P. J. Verkerk, T. Kuemmerle, Archetypical patterns and trajectories of land systems in Europe. *Reg. Environ. Change* **18**, 715–732 (2018).

65. H. Yin, V. Butsic, J. Buchner, T. Kuemmerle, A. V. Prishchepov, M. Baumann, E. V. Bragina, H. Sayadyan, V. C. Radeloff, Agricultural abandonment and re-cultivation during and after the Chechen Wars in the northern Caucasus. *Glob. Environ. Change* **55**, 149–159 (2019).

66. A. V. Prishchepov, D. Müller, M. Dubinin, M. Baumann, V. C. Radeloff, Determinants of agricultural land abandonment in post-Soviet European Russia. *Land Use Policy* **30**, 873–884 (2013).

67. A. Smaliychuk, D. Müller, A. V. Prishchepov, C. Levers, I. Kruhlov, T. Kuemmerle, Recultivation of abandoned agricultural lands in Ukraine: Patterns and drivers. *Glob. Environ. Change* **38**, 70–81 (2016).

68. F. Hua, X. Wang, X. Zheng, B. Fisher, L. Wang, J. Zhu, Y. Tang, D. W. Yu, D. S. Wilcove, Opportunities for biodiversity gains under the world's largest reforestation programme. *Nat. Commun.* **7**, 12717 (2016).

69. H. Yin, D. Pflugmacher, A. Li, Z. Li, P. Hostert, Land use and land cover change in Inner Mongolia—Understanding the effects of China's re-vegetation programs. *Remote Sens. Environ.* **204**, 918–930 (2018).

70. V. M. Olsen, R. Fensholt, P. Olofsson, R. Bonifacio, V. Butsic, D. Druce, D. Ray, A. V. Prishchepov, The impact of conflict-driven cropland abandonment on food insecurity in South Sudan revealed using satellite remote sensing. *Nat. Food* **2**, 990–996 (2021).

71. A. V. Prishchepov, E. V. Ponkina, Z. Sun, M. Bavorova, O. A. Yekimovskaja, Revealing the intentions of farmers to recultivate abandoned farmland: A case study of the Buryat Republic in Russia. *Land Use Policy* **107**, 105513 (2021).

72. E. A. Coleman, B. Schultz, V. Ramprasad, H. Fischer, P. Rana, A. M. Filippi, B. Güneralp, A. Ma, C. Rodriguez Solorzano, V. Guleria, R. Rana, F. Fleischman, Limited effects of tree planting on forest canopy cover and rural livelihoods in Northern India. *Nat. Sustain.* **4**, 997–1004 (2021).

73. Food and Agriculture Organization of the United Nations (FAO), FAOSTAT Statistical Database: Methods & Standards (2016); www.fao.org/ag/agn/nutrition/Indicatorsfiles/Agriculture.pdf.

74. RStudio Team, RStudio: Integrated Development Environment for R (2020); www.rstudio.com/.

75. R Core Team, R: A language and environment for statistical computing (R Foundation for Statistical Computing, 2021); www.r-project.org/.

76. R. J. Hijmans, Terra: Spatial data analysis (2022); https://rspatial.org/terra/.

77. M. Dowle, A. Srinivasan, Data.table: Extension of 'data.frame' (2021); http://r-datatable.com/.

78. H. Wickham, Tidyverse: Easily install and load the tidyverse (2021); www.tidyverse.org/.

79. E. Dinerstein, D. Olson, A. Joshi, C. Vynne, N. D. Burgess, E. Wikramanayake, N. Hahn, S. Palminteri, P. Hedao, R. Noss, M. Hansen, H. Locke, E. C. Ellis, B. Jones, C. V. Barber, R. Hayes, C. Kormos, V. Martin, E. Crist, W. Sechrest, L. Price, J. E. M. Baillie, D. Weeden, K. Suckling, C. Davis, N. Sizer, R. Moore, D. Thau, T. Birch, P. Potapov, S. Turubanova, A. Tyukavina, N. De Souza, L. Pintea, J. C. Brito, O. A. Llewellyn, A. G. Miller, A. Patzelt, S. A. Ghazanfar, J. Timberlake, H. Klöser, Y. Shennan-Farpón, R. Kindt, J. P. B. Lillesø, P. Van Breugel, L. Graudal, M. Voge, K. F. Al-Shammari, M. Saleem, An ecoregion-based approach to protecting half the terrestrial realm. *BioScience* **67**, 534–545 (2017).

80. D. A. Bossio, S. C. Cook-Patton, P. W. Ellis, J. Fargione, J. Sanderman, P. Smith, S. Wood, R. J. Zomer, M. von Unger, I. M. Emmer, B. W. Griscom, The role of soil carbon in natural climate solutions. *Nat. Sustain.* **3**, 391–398 (2020).

81. P. Legendre, L. Legendre, *Numerical Ecology* (Elsevier, ed. 3, 2012).